On the resolution function of the n_TOF facility: a comprehensive study and user guide

V. Vlachoudis[1], M. Sabaté-Gilarte[1,2],
V. Alcayne[3], F. Gunsing[4], E. Mendoza[3], F. Ogallar[1], I. Rejwan*,
M. Bacak[5], C. Guerrero[2], C. Massimi[7,8], A. Stamatopoulos[9]

[1]CERN (Switzerland), [2]University of Seville (Spain),
[3]CIEMAT (Spain), [4]CEA-Saclay (France), [5]PSI (Switzerland), [7]INFN (Italy),
[8]University of Bologna (Italy), [9]LANL (USA), *Summer Student 2018

Vasilis.Vlachoudis@cern.ch
marta.sabate.gilarte@cern.ch

n_TOF-PUB-2021-001
16/04/2021

Friday 16th April, 2021

Contents

Abstract

The purpose of this report is to provide the necessary information and tools for the n_TOF Collaboration [1] on how to correctly account for the neutron resolution function in the experimental areas (EAR1 and EAR2) for different n_TOF operation periods.

The n_TOF target as well as the cooling/moderation system was designed to optimize the performances of the neutron beam for EAR1 [2]. Additionally, EAR1 is located underground 200 m away, in nearly the same direction as the incoming proton beam, from the spallation target. On the contrary, EAR2 [3] was an extension of the existing facility. It is located above the ground at 20 m from the spallation target in the perpendicular direction with respect to the incoming proton beam. Even though the energy resolution is worse due to the shorter flight path, the main issue with the resolution function comes from the geometry of the cooling/moderation system and the shape of the spallation target.

Experimental data acquired in any of the experimental areas has embedded the effect of the resolution function. Therefore, when treating these data there are two options. Either deconvolute them from the resolution function or convolve the reference data, for instance evaluated cross sections, with the resolution function to be able to compare both sets of data in the same conditions. Usually, the second method is adopted for simplicity. In both cases the explicit distribution of the resolution function should be available. Even more, to perform the resonance analysis with SAMMY [4] or REFIT [5] this information must be known.

The question here is: how to obtain the resolution function.

Chapter 1

Resolution Function: an overview

The Resolution Function (RF) is the name used to designate the distribution that correlates measured neutron time-of-flight (TOF) with the neutron energy. The function that described this relationship is rather a distribution than a one-to-one constant as illustrated in Figure 1.1. Neutrons reaching the experimental hall at a given TOF have an energy distribution (and vice versa) which is highly non-Gaussian, except at high neutron energies where the dominant contribution comes from the width of the primary proton burst.

The RF is determined via the Monte Carlo simulations of the spallation and cooling/moderation processes (see Chapter 1.1). Figure 1.1 is an example of FLUKA [6] simulations at 1.5 m above the spallation target. Neutrons lose their energy due to successive scatterings in the materials that they find on their way. The definition of the RF as shown in Figure 1.1 is not satisfactory since the TOF and neutron energy ranges are too wide to provide a suitable representative number of bins in the histogram, which entails a significant loss of information. Therefore, this representation is replaced by an equivalent one but in terms of TOF and λ (Figure 1.2), where $\lambda = v \cdot t$. It is not the real distance rather the effective flight path as appears at the time of evaluation.

The study of the RF in terms of λ allows us to express the RF as a correction to the flight path in the conversion from TOF to energy. In this picture, the flight path is made of two components: the geometrical distance from the center of the spallation target to the sample position (L_0) and the additional flight path due to

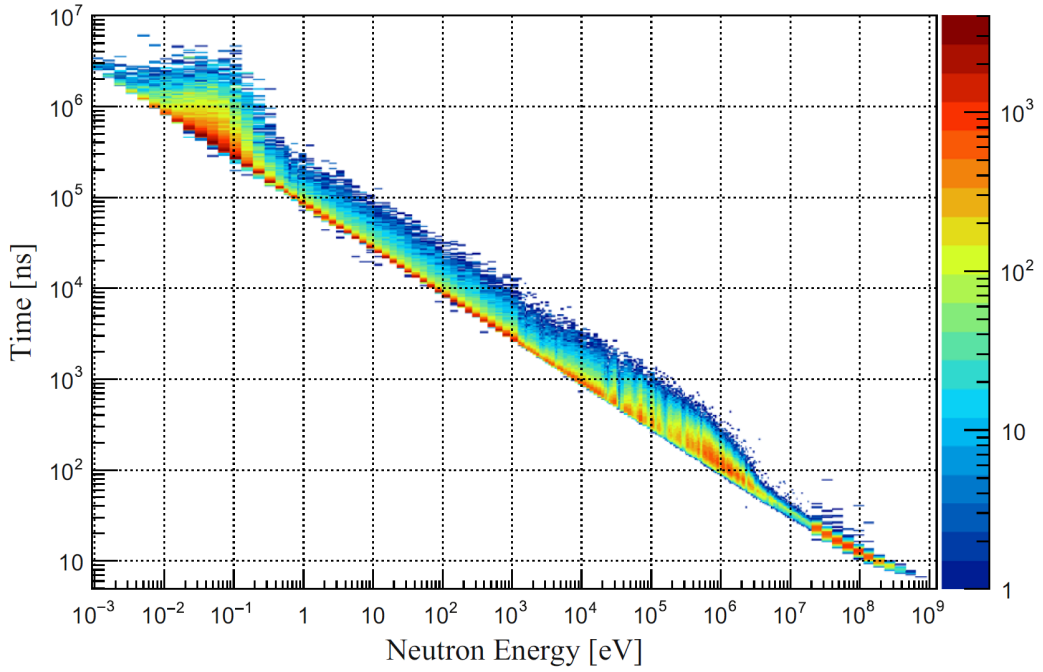

Figure 1.1: FLUKA simulations of the relationship between time-of-flight and neutron energy above 1.5 m from the spallation target. The width of the proton burst is not included in this plot (source [7]). Arbitrary units in Z-axis.

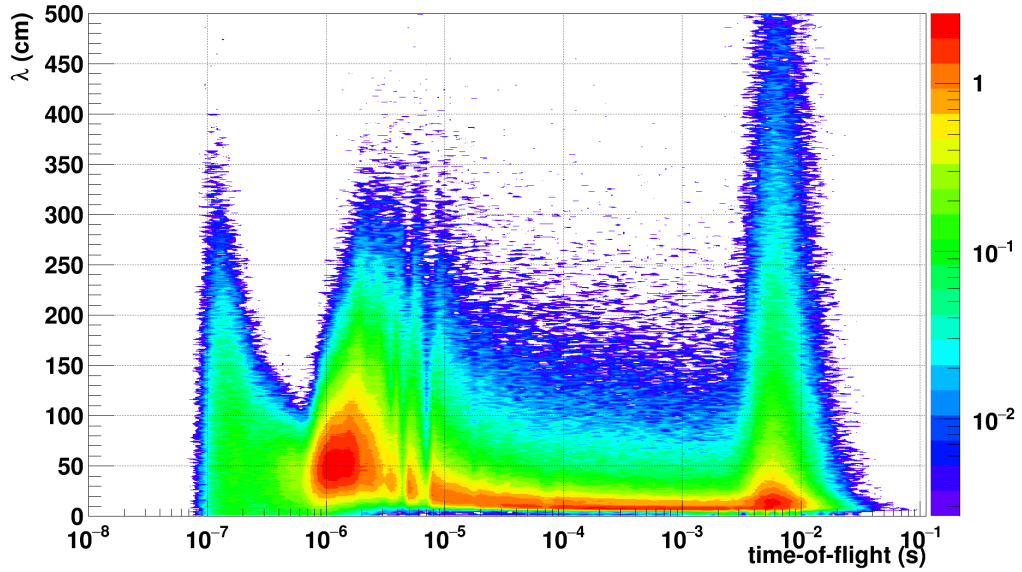

Figure 1.2: TOF vs. λ for n_TOF-Phase3 EAR2 at 19.3 m from the spallation target. Arbitrary units in Z-axis [8].

successive interactions of neutrons inside the target and the cooling/moderation volume ($\lambda(E)$ or $\lambda(TOF)$). Therefore, the flight path can be expressed as $L = L_0 + \lambda$ (Eq. 4.7). For simplicity, instead of including the full λ-distribution, a representative value of it can be used instead (Eq. 4.10). Figure 1.3 shows the mean and maximum value of the RF distribution as a function of the TOF. Even though mathematically a suitable parameter to represent the distribution is the mean value, it highly relies on how well the physics model is implemented in the simulations, i.e., how good the tail of the distribution is treated. Besides, as observed, the mean and the maximum values show different behaviour as a function of the TOF for n_TOF-EAR2. Therefore, no representative value of the distribution should be used in this way.

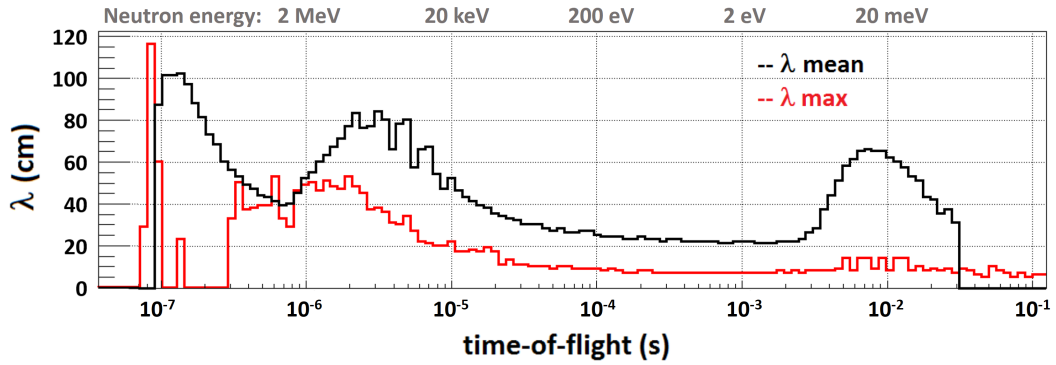

Figure 1.3: The projection of the RF in various TOF ranges enables the calculation of the maximum (red) and the mean (black) value of the distribution. As can be observed, they exhibit different behaviour [8].

The solution to this problem would be the use of the complete λ-distribution in the TOF to E conversion. However, it was observed that a constant representative value of this distribution can be used in a given neutron energy range which strongly depends on the experimental set-up, i.e., sample geometry, alignment, sample location with respect to the spallation target, etc. **This representative value is unique for each experiment and can be obtained by means of the available *Transport Code* (Chapter 3).**

1.1 FLUKA+MCNP simulations

The n_TOF neutron beam energy spectrum is very wide, comprising energies from sub-thermal (< 25 meV) up to a few GeV. The way neutrons are transported in FLUKA [6] depends on their energy. Above 20 MeV physics models are considered. However, below certain values the transport is performed by a multi-group algorithm. The cross section library contains 260-groups for energies below 20 MeV. Nevertheless, this method introduces artifacts in the neutron beam features extracted from the simulations, such as the neutron flux or the RF (see Figure 1.4). Maxwellian smoothing can correct the neutron fluence but not the RF. Contrary to this approach, MCNP [9] applies the point-wise cross section libraries below 20 MeV, avoiding the artifacts and providing better resolution along the energy range since the energy intervals are not grouped. Therefore coupled simulations FLUKA+MCNP were performed instead: the spallation process and all particles are tracked in FLUKA, except neutrons with energies <20 MeV which are tracked by MCNPx v2.6.0. Both sets of simulations implement the same geometry. The CPU time needed to reach the same number of primary protons is twice the time needed in past FLUKA-based simulations [10].

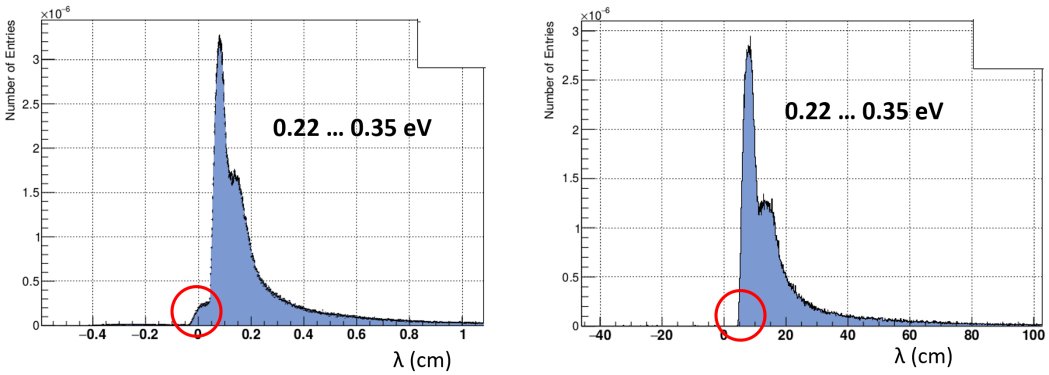

Figure 1.4: λ distribution (a.u. in X and Y axis) projected in the neutron energy range from 0.22 to 0.35 eV extracted from FLUKA simulations (left) and from the coupled FLUKA plus MCNP simulations (right) [11]. The spike on the left side of the peak is an artifact that appears when using the group cross section approach in FLUKA; it disappears when neutrons with energies below 20 MeV are transported by MCNP instead of by FLUKA.

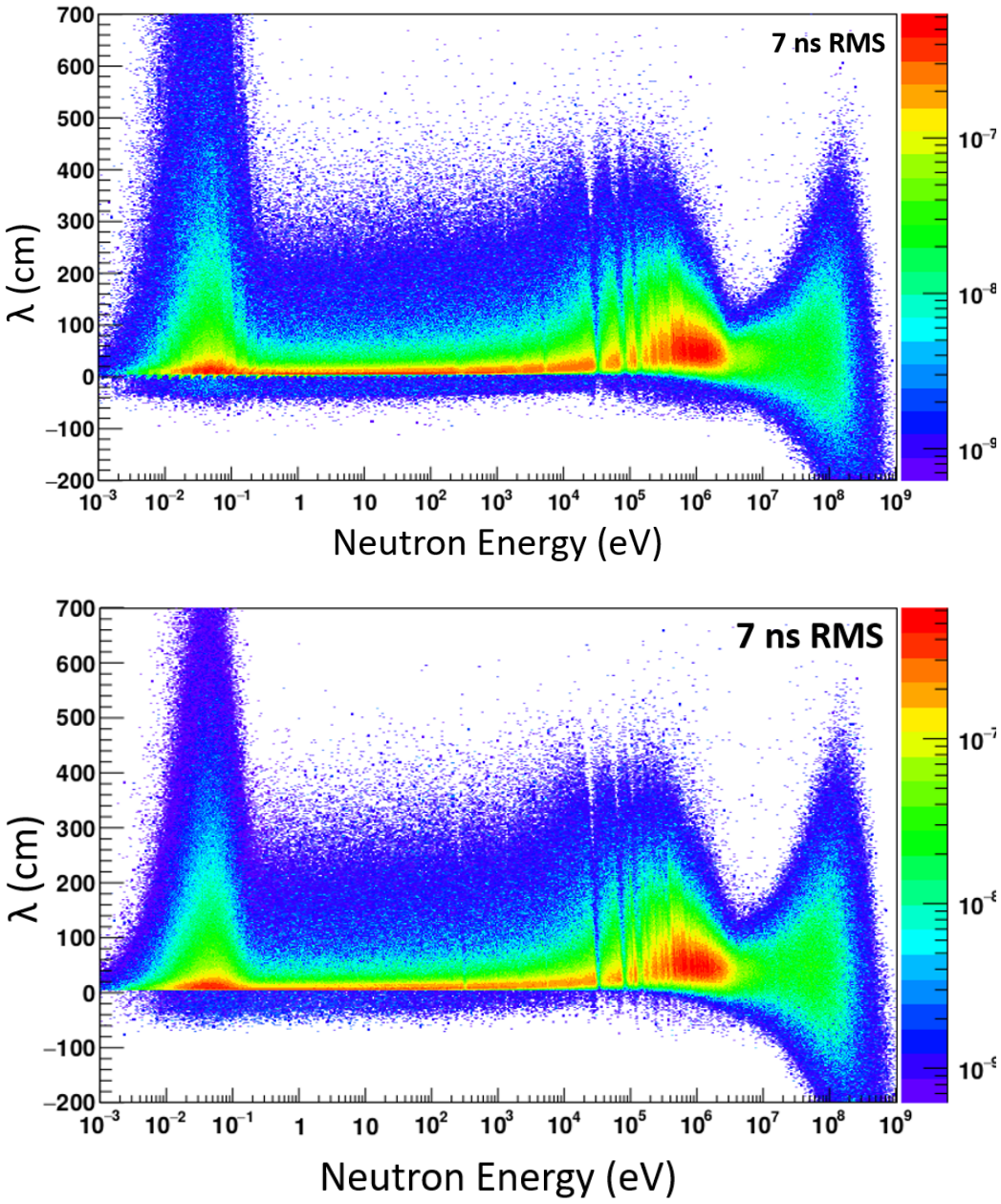

Figure 1.5: λ 2D-distribution (a.u. in Z-axis) as a function of the neutron energy obtained from FLUKA simulations (top) and from the coupled FLUKA plus MCNP simulations (bottom) [11]. The spikes below $\lambda = 0$ in the first distribution are artifacts due to the use of the group cross section approach in FLUKA, they disappear when neutrons with energies below 20 MeV are transported with MCNP.

Chapter 2

Data treatment: A particular RF for each experiment

The RF is extracted from the coupled FLUKA and MCNP simulations. As already mentioned, the first code tracks all particles but neutrons with energies below 20 MeV which are tracked by MCNP instead. The scoring is located at the exit of the moderator. In case of EAR1, the scoring plane is exactly after the support structures of the vacuum chamber window, which is at approximately 41 cm. For EAR2, the scoring plane is defined at 37.2 cm from the target center in the vertical direction. However, due to the non-optimized geometry of the target and cooling/moderation system for EAR2, neutrons can reach the scoring plane from the sides of the vacuum chamber as well as from the step in the cooling/moderation circuit at 1.5 m, what has a great impact on the shape of the RF. From the scoring location to the sample position, neutrons are optically transported using a dedicated code, which allows us to select the sample size, the offset with respect to the centre of the beam and the flight path as input.

The method to check the quality of the calculations consists on reproducing the count rate or the yield of a set of reference measurements, whose cross sections are well characterized. For instance, (n,γ) reactions with well known resonances in different energy regions. Evaluated data have to be folded with the RF in order to better replicate the expected count rate. A proposed procedure is to profit from the features of the *Transport Code*. From this code not only the characteristics

of the neutron beam from the simulations, such as the flux or the RF, can be obtained. It also offers a technique to reproduce experimental conditions from evaluated data.

The RF for an experimental area is obtained by means of the *Transport Code*. One of the main inputs to run the code is the flight path. If, with a unique value of it, the RF reproduces in a proper way the cross section resonances of any measured reaction in that experimental area, then that RF and the used flight path become the reference parameters for data analysis. This is the case of EAR1 for which a unique flight path (185 m) is considered to extract the RF. Nevertheless, the RF of EAR2 is very sensitive to the flight path value. Meaning that a variation of few tens of mm implies a change in the shape of the RF distribution. Therefore, the convolution of evaluated data with the RF will differ. **Consequently, for EAR2 there is not a general RF for all experiments rather than a unique one for each of them**. Even more, the RF also depends on the size and shape of the sample as well as on its alignment with respect to the beam position. Once more, these effects appear to be negligible for EAR1, located at 185 m from the target, but it has a important impact in EAR2, at 20 m from the target. Figure 2.1 shows the spatial distribution of the beam at different positions in EAR2. The shape of the beam profile changes quite fast with the height. As a result, we have to differentiate between *Large samples*, those that cover the whole beam profile, and *Small samples* which only cover a portion of it. The *Beam Intersection Factor* correction is not enough in EAR2 to account for the effect of not covering the full beam as in case of EAR1.

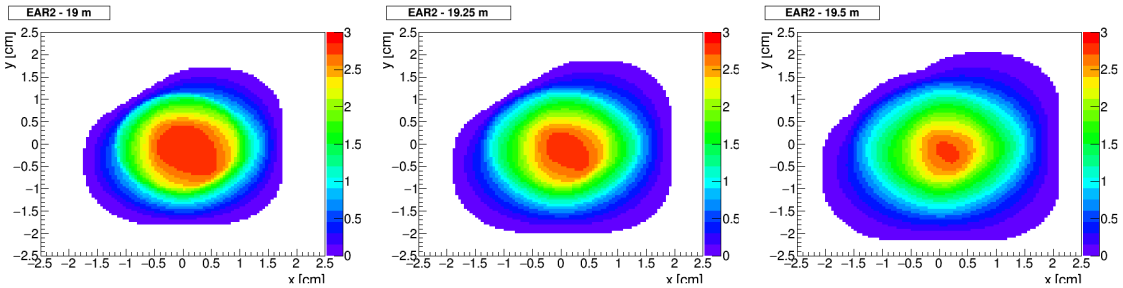

Figure 2.1: EAR2 beam profile at 19 m, 19.25 m and 19.5 m from the spallation target for all neutron energies.

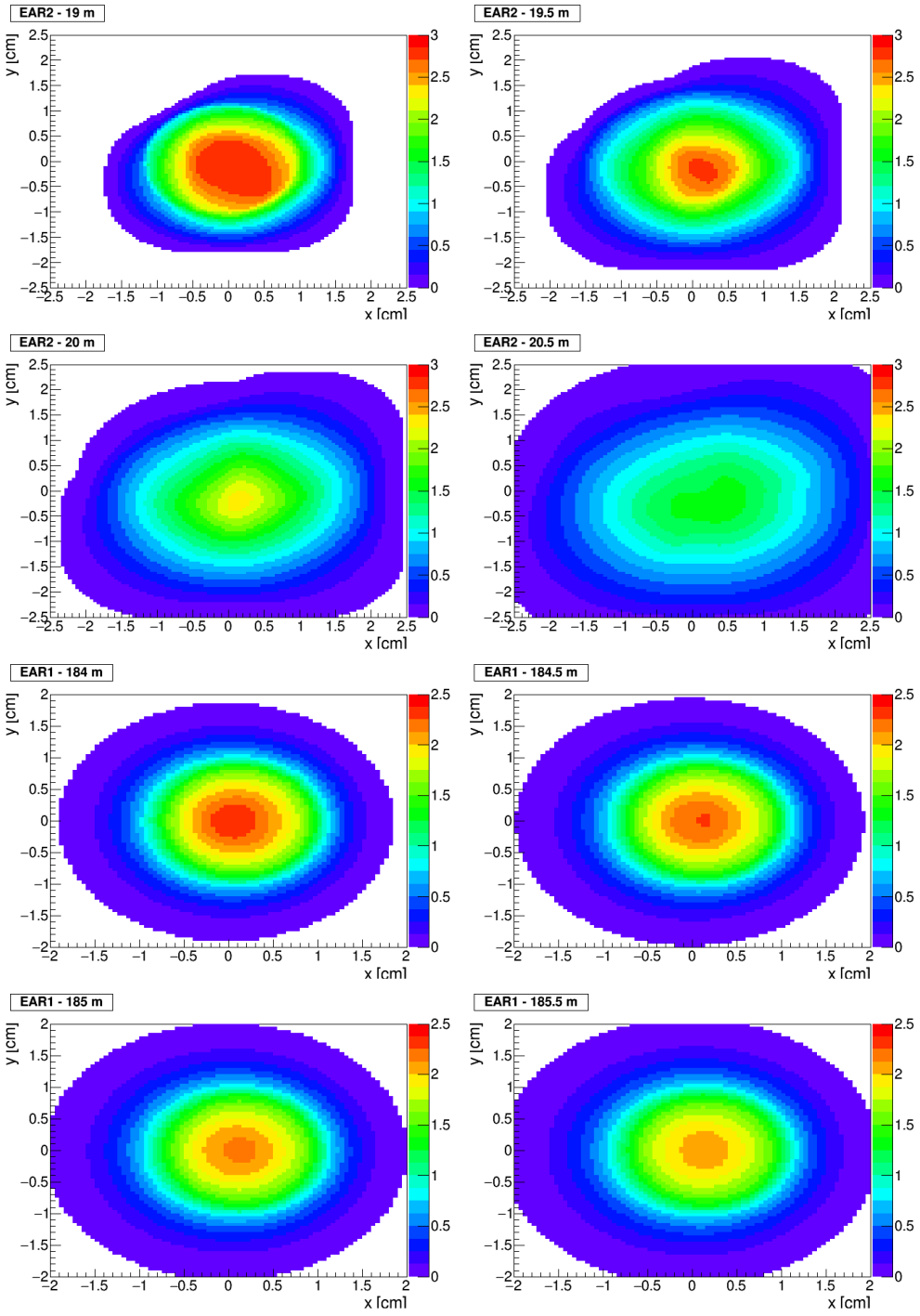

Figure 2.2: Top 4 plots: EAR2 beam profile at 19 m, 19.5 m, 20 m and 20.5 m. Bottom 4 plots: EAR1 beam profile at 184 m, 184.5 m, 185 m and 185.5 m.

Large samples are those samples that cover the entire beam profile at all neutron energies. The results of the comparison of experimental data with the evaluated data convoluted with the RF is shown in Figures 2.3 and 2.4. There is a perfect reproduction of the count rate over the whole TOF range. Therefore, the RF can be directly extracted by adjusting only the flight path for each sample.

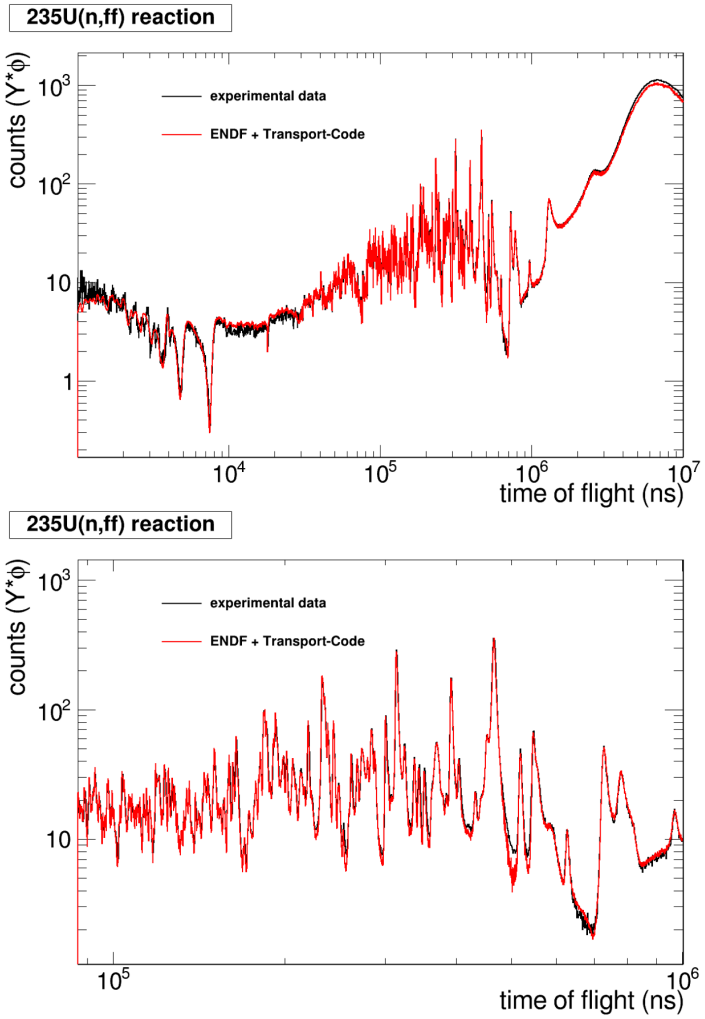

Figure 2.3: Fission count rate of $^{235}U(n,ff)$ as a function of TOF in different energy ranges. The experimental data (black) was obtained from a measurement with μMGAS detector loaded with 90 mm diameter ^{235}U sample at n_TOF-EAR2. The evaluated data, ENDF-VII.1 (red), is already convoluted with the RF of n_TOF-EAR2 [10].

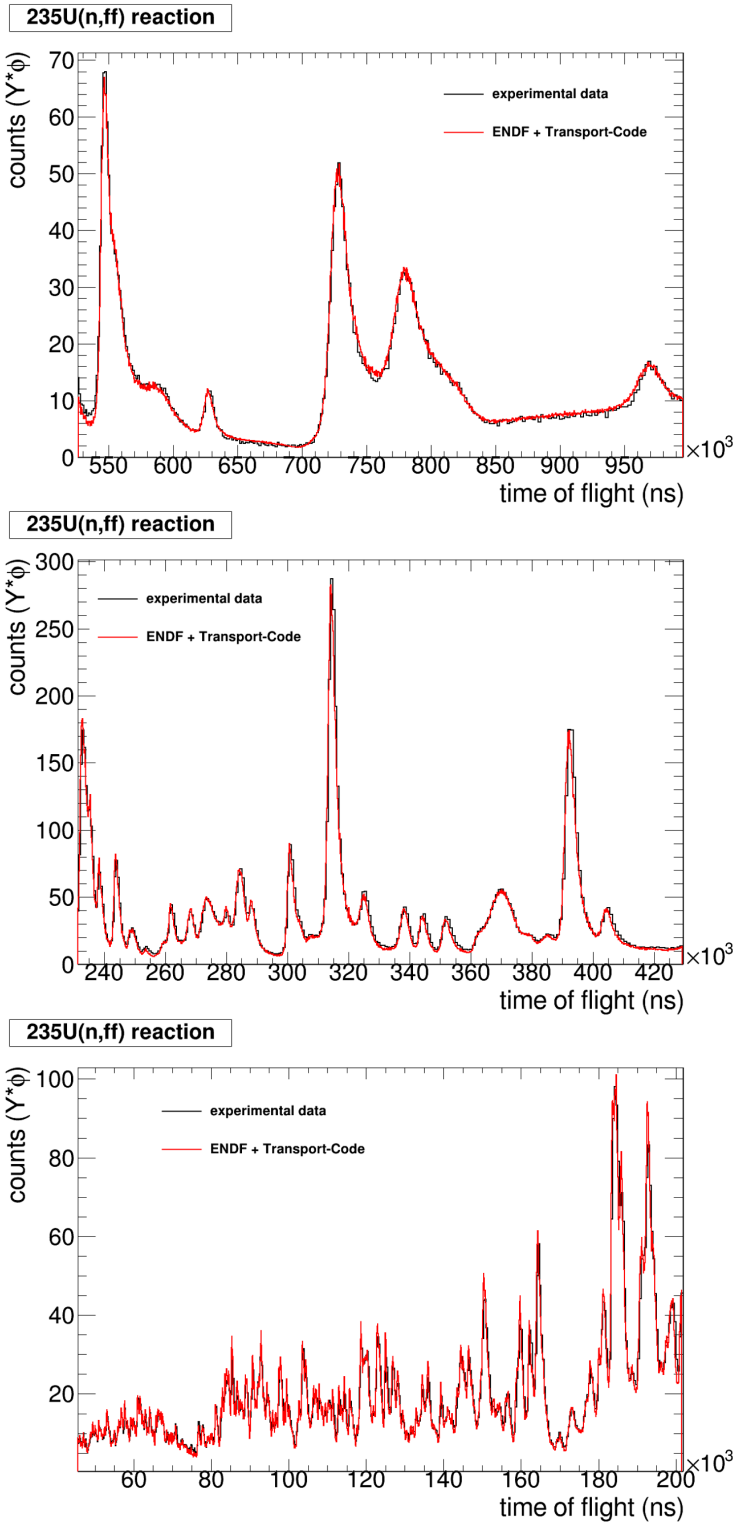

Figure 2.4: Continuation of Figure 2.3.

Very small samples: contrary to previous case, this category applies to samples that only cover a fraction of the beam profile, and/or that are not necessarily well aligned with respect to the incoming neutron beam. Since there is a clear dependency of the RF with the geometry and alignment of the sample, in addition to the flight-path, a different procedure to get the RF must be followed. Even though what we present here is a limit case in which the size of the sample was specially small (2.5 mm in radius), the methodology can be applied to all small samples. Although, the last step of this method, in which a parametrization of the RF for different energy ranges is needed, may not be necessary for bigger samples.

During the Cm campaign in 2017 a very small ^{197}Au sample with a radius of 2.5 mm was measured in EAR2 with BICRON detectors, a kind of liquid scintillator, in the range between 0.1 to 300 eV. The method explained in Chapter 3 was used to obtain the RF and the time-of-flight distance. In this particular case, the sample was misaligned by one or two millimetres with respect to the centre of the beam. Various RFs with different misalignment values were studied and the one that better reproduces the data was taken as the final RF. In Figure 2.5, the two yields obtained using this RF and a RF for a sample covering the whole beam are compared with the experimental yield. See [12, 13] for more details. There is an important improvement in the RF when the optical *Transport Code* is used. However, the quality of the RF is not good enough to perform resonance analysis as can be seen in Figure 2.6 and Tables 2.1, 2.2 and 2.3. The work done to further improve the RF consists on parametrizing the RF obtained with the *Transport Code* with a combination of Gaussian, Landau and Exponential functions (see Figure 2.7). After the parametrization, the ratio between the different functions is adjusted to better replicate the ^{197}Au(n,γ) resonances. The parameters extracted for each resonance are interpolated to obtain the RF in the range between 0.1 to 300 eV. In Figure 2.8, the new RF calculated with the fit is shown as well as the RF obtained with the *Transport Code*. In Figure 2.9 the λ distributions from the *Transport Code* is compared with the fit for several neutron energies. With the adjusted RF using this method, the resonance parameters replicate in a more accurate way the evaluated values of the library JEFF 3.3. In particular the Γ_γ parameters calculated with the new RF are compatible with the evaluated JEFF 3.3, except for those at around 150 eV that deviates by 30%.

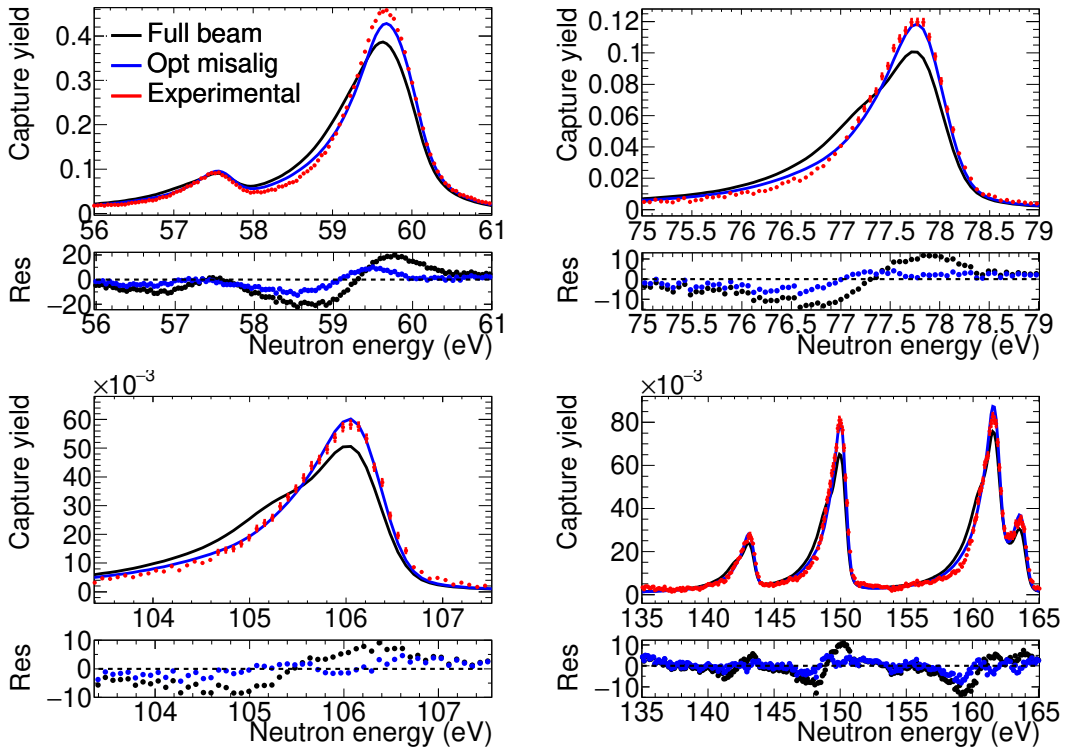

Figure 2.5: The experimental $^{197}Au(n,\gamma)$ yield for a circular sample of 2.5 mm radius (red) compared with two yields obtained with SAMMY using the RF calculated for large samples (black) and for the RF adjusted for a 2.5 mm radius circular sample misalignment (blue). In the lower part of each image the residuals are plotted.

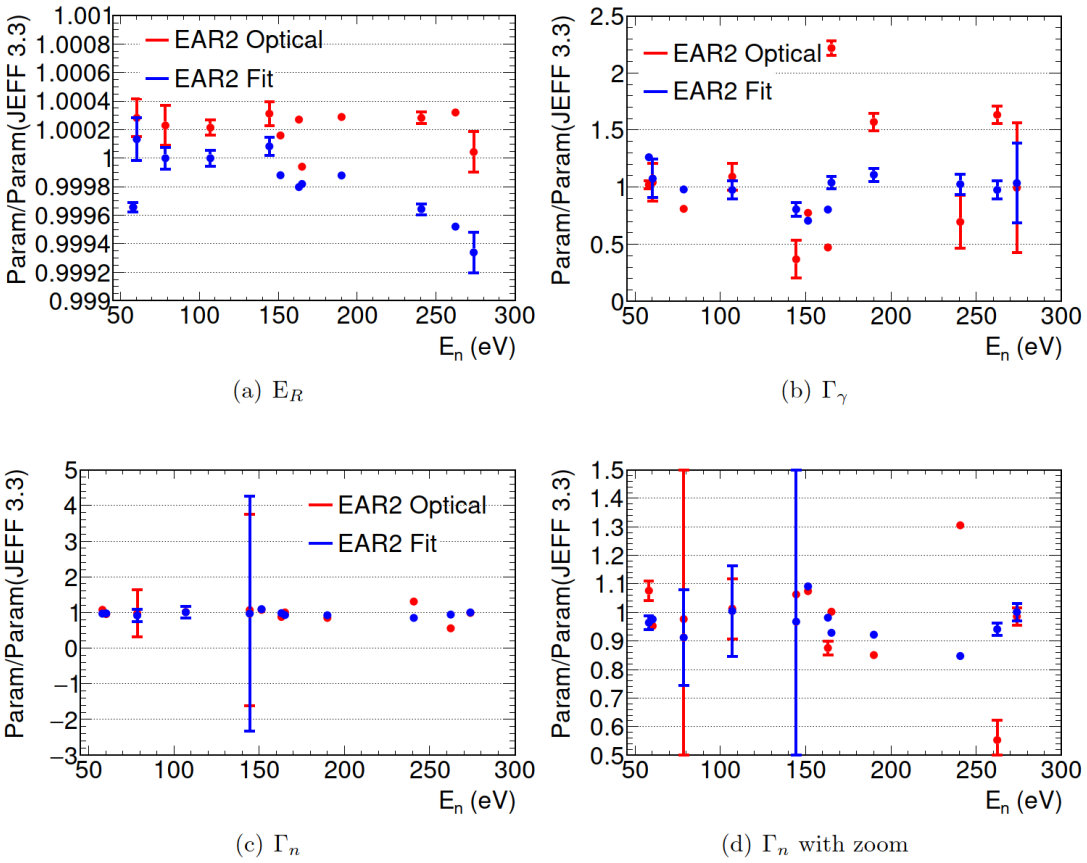

(a) E_R (b) Γ_γ

(c) Γ_n (d) Γ_n with zoom

Figure 2.6: The resonance parameter obtained in the analysis of the $^{197}Au(n,\gamma)$ done with SAMMY are compared with the JEFF 3.3 evaluated data. In red, the parameters obtained with the yield measured in EAR2 with the C_6D_6 including in SAMMY the RF as extracted from the Transport Code, considering the sample size and its misalignment with respect to the beam center. In blue, the fitted RF. The error bars refer only to statistical uncertainties.

E_R			
E_R	Evaluated JEFF 3.3	EAR2 Optical transport	EAR2 Fit
58	58.08	58.06 ± 0.00	58.06 ± 0.00
60	60.29	60.31 ± 0.01	60.30 ± 0.01
79	78.50	78.52 ± 0.01	78.50 ± 0.01
107	107.03	107.06 ± 0.01	107.03 ± 0.01
144	144.41	144.45 ± 0.01	144.42 ± 0.01
151	151.39	151.42 ± 0.00	151.37 ± 0.00
163	163.07	163.11 ± 0.00	163.03 ± 0.00
165	165.08	165.07 ± 0.00	165.05 ± 0.00
190	190.03	190.09 ± 0.00	190.01 ± 0.00
241	240.61	240.68 ± 0.01	240.52 ± 0.01
262	262.26	262.35 ± 0.01	262.14 ± 0.01
274	273.86	273.87 ± 0.04	273.68 ± 0.04

Table 2.1: The E_R parameter from the resonance parameters analysis done with SAMMY for the $^{197}Au(n,\gamma)$ yield. The second column corresponds to the evaluated database JEFF 3.3. The third column is obtained using the RF calculated with the Optical Transport Code and the fourth with the RF calculated with the Fit. The uncertainties in the table only account for the statistical uncertainties.

Γ_γ			
E_R	Evaluated JEFF 3.3	EAR2 Optical transport	EAR2 Fit
58	113	115 ± 4	143 ± 4
60	118	123 ± 20	127 ± 20
79	124	101 ± 1	122 ± 3
107	123	134 ± 15	120 ± 10
144	121	45 ± 20	98 ± 7
151	121	94 ± 0	85 ± 0
163	129	61 ± 3	104 ± 2
165	121	269 ± 8	126 ± 7
190	121	190 ± 9	134 ± 7
241	121	84 ± 28	124 ± 11
262	129	211 ± 10	126 ± 10
274	121	120 ± 69	125 ± 42

Table 2.2: The Γ_γ parameter from the resonance parameters analysis done with SAMMY for the $^{197}Au(n,\gamma)$ yield. The second column corresponds to the evaluated database JEFF 3.3. The third column is obtained using the RF calculated with the Optical Transport Code and the fourth with the RF calculated with the Fit. The uncertainties in the table only account for the statistical uncertainties.

Γ_n			
E_R	Evaluated JEFF 3.3	EAR2 Optical transport	EAR2 Fit
58	4.3	4.6 ± 0.1	4.2 ± 0.1
60	70.7	67.3 ± 0.8	68.9 ± 0.1
79	17.0	16.6 ± 11.1	15.5 ± 2.8
107	7.8	7.9 ± 0.8	7.9 ± 1.3
144	9.1	9.6 ± 24.4	8.8 ± 19.8
151	22.3	23.9 ± 0.0	24.3 ± 0.0
163	55.2	48.3 ± 1.4	54.1 ± 0.2
165	10.0	10.0 ± 0.1	9.3 ± 0.1
190	49.1	41.7 ± 0.7	45.2 ± 0.7
241	74.2	96.8 ± 0.2	62.8 ± 0.1
262	144.0	79.6 ± 10.2	135.5 ± 3.1
274	4.8	4.8 ± 0.1	4.8 ± 0.1

Table 2.3: The Γ_n parameter from the resonance parameters analysis done with SAMMY for the $^{197}Au(n,\gamma)$ yield. The second column corresponds to the evaluated database JEFF 3.3. The third column is obtained using the RF calculated with the Optical Transport Code and the fourth with the RF calculated with the Fit. The uncertainties in the table only account for the statistical uncertainties.

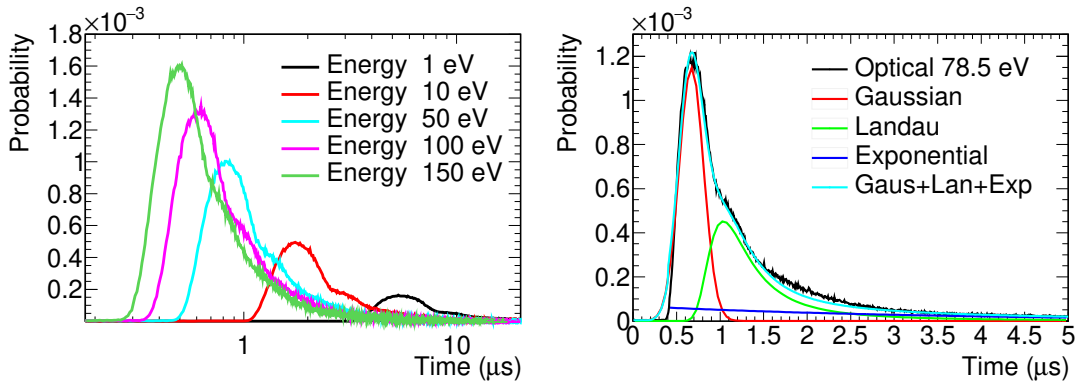

Figure 2.7: On the left, λ distribution for several neutron energies. On the right, λ distribution at 78.5 eV from the optical transport (black) and the fitted one (clear blue) with a combination of Gaussian (red), Landau (green) and Exponential (blue) functions.

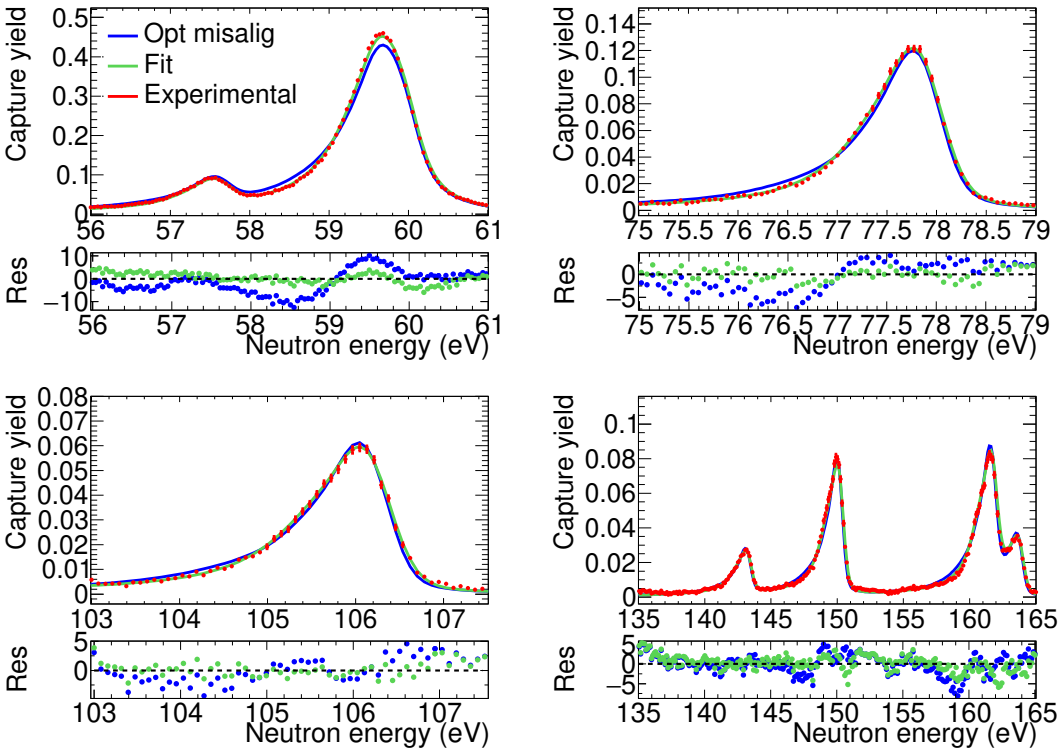

Figure 2.8: The experimental $^{197}Au(n,\gamma)$ yield (red) for a circular sample with 2.5 mm radius is compared with the two yields calculated with SAMMY with the RF for a 2.5 mm circular sample misalignment by 1.8 mm to optimize the fit (green) and the RF calculated by fitting each $^{197}Au(n,\gamma)$ resonance and the first of the $^{244}Cm(n,\gamma)$ reaction. In the lower panel of each image the residuals are plotted.

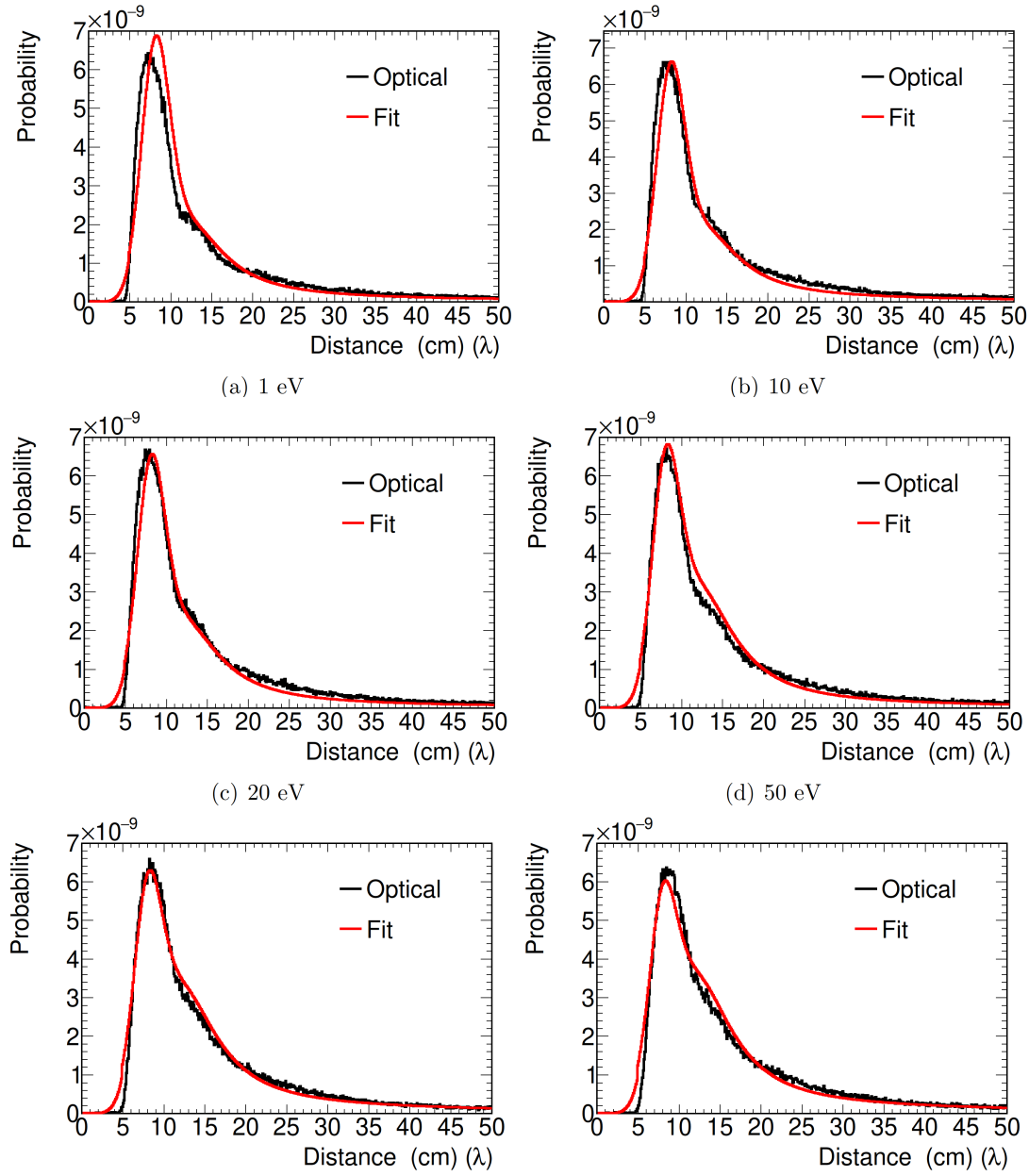

(a) 1 eV (b) 10 eV

(c) 20 eV (d) 50 eV

(e) 100 eV (f) 150 eV

Figure 2.9: The comparison of the λ distributions of the EAR2 RF for different neutron energies. The black line are the distributions obtained with the Optical Transport Code and the misalignment. The red line are the distributions from the fit of the $^{197}Au(n,\gamma)$ resonances and the $^{244}Cm(n,\gamma)$ first resonance.

Conclusions: In view of these results for large and small samples, whose analysis were carried out by CERN and CIEMAT teams, the following conclusions can be extracted regarding the RF of EAR2:

- The coupled simulations of FLUKA+MCNP provides a reliable EAR2-RF.
- Two experimental data sets were used to check the quality of the obtained RF. This process has shown that it is not possible to apply the same RF to all experimental cases since it critically depends on the flight path as well as on the geometry and alignment of the sample.
- The flight path needed in the TOF to energy conversion for each experiment has to be extracted using a reference sample with well known resonances. The comparison is done in TOF. Using the *Transport Code* one can fold the evaluated cross section, given in terms of neutron energy, to obtain the expected count rate in TOF. Then it is possible to compare experimental data with the evaluation.
- Since the RF varies significantly with the value of the flight path, the resonance analysis of an experiment carried out with a detector loaded with multiple samples may need different RF: to be checked by the user.
- For small samples, in addition to the flight path, the sample geometry and its position with respect to the neutron beam should be adjusted as well. Once more, the *Transport Code* turns out to be the most reliable method to get the optimum parameters prior extracting the RF for a given experiment.
- For very small samples, the quality of the RF is not enough to successfully perform the resonance analysis. The method proposed here is to find the best fit of the λ distribution for different neutron energy ranges for the resonances of the reference reaction cross section, for instance ^{197}Au(n,γ). What introduces a higher level of complexity.

A specific RF is needed for each detector configuration or cross section measurement. The search for the most reliable form of the RF is the duty of the measurement responsible since they are fully aware of the measurements details such as alignment, number of samples, distance between the sample of interests and the reference one, etc.

Chapter 3

How to obtain the Resolution Function: the Transport Code

The *Transport Code* is an optical transport routine, coded in C++, designed to project the neutron positions from one surface to another considering any obstacle between them that can affect neutron tracks, like collimators or beam pipe reductions. Object locations and their dimensions are based on the technical drawings of the facility. Assuming that the angular distribution is isotropic within an angle θ, neutrons are projected to a surface at distance L from the original plane except those which are outside the circle defined by $L_0 \cdot tan(\theta) - \rho$, where ρ is the aperture of the first tube in the line included in order to remove the beam halo created from an extended source [14]. Neutron trajectories are calculated from the original scoring plane, the one which contains the information from simulations, to every point in the new surface. The trajectories that do not fulfill the collimation conditions are discarded. For the rest of them, the new coordinates and directions are assigned [14]. Schematically, Figures 3.1 and 3.2 show the scoring planes involved on simulations and optical transport.

This method is a way of folding a given cross section with the λ distribution. What can be obtained as output depends on the input definition. If the total/partial cross section of the reaction under study together with the areal density of the deposit is provided, the expected count rate is obtained in terms of the time-of-flight or the true-energy. Furthermore, if the efficiency of the detec-

tion system and the transmission factors, cross section and areal density of any material in-beam, are included as a function of the neutron energy, the resulted count rate will be affected by all these effects at the same time that the evaluated cross sections used for calculating these factors is folded with the response function.

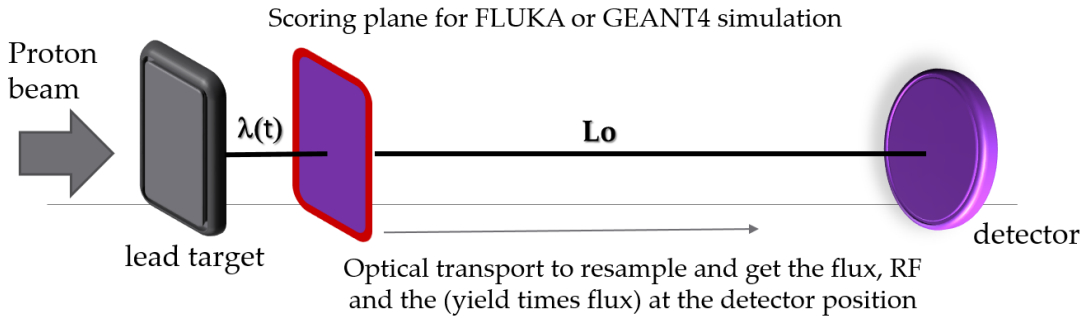

Figure 3.1: Scheme of the neutron transport principle from Monte Carlo simulation scoring plane to the final surface located at L_0 from the previous one [8].

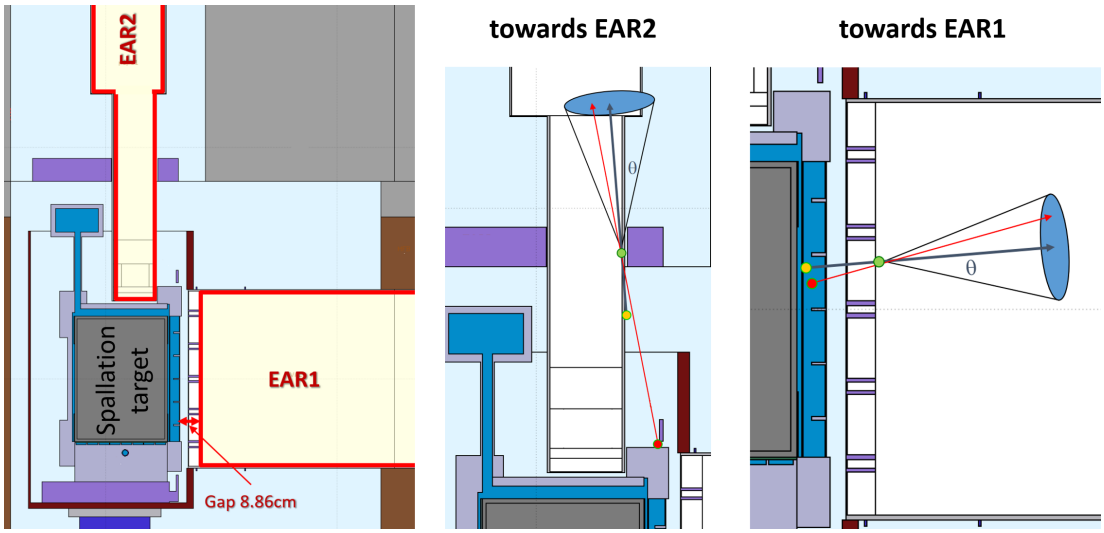

Figure 3.2: Geometry of the target area as implemented in FLUKA. Left: the spallation target is shown, the vacuum lines towards the experimental areas are highlighted. Angular acceptance for the optical transport from the scoring plane towards the EAR2 (middle) and EAR1 (right) [17].

In order to perform the resonance analysis with SAMMY, the RF has to be provided either using its analytical form or by means of its numerical representation. In both cases the distribution should be given as a function of the neutron energy together with the estimated flight path to ensure a proper TOF to neutron energy conversion.

The *Transport Code* is a tool that helps to extract the needed parameters to produce the correct RF, with the same script, for a particular experiment. The starting point is the known information such as the preliminary flight path, sample properties and evaluated cross sections. This information used as input allows one to compare the experimental count rate with the expected one from the evaluations, in case of reference samples, in terms of TOF. The reason why it is better to carry out the search for the good parameters in term of TOF instead of neutron energy is to avoid the transformation of the experimental TOF, which implies one of the parameters to be adjusted: the flight path. From the comparison of both sets of data one can observe the differences in the shape and location of the resonances due to a wrong flight path, the misalignment of the sample or even the sample mass. Therefore, the input parameters are modified to better match the experimental data. As shown, it is an iterative process for several variables. The number of iterations depends on how much off the initial information is with respect to the real experimental conditions. Once the iterative process converges, i.e., when the expected count rate perfectly fits the experimental one in TOF, the final set of parameters serves as input to produce the file with the RF as a function of the neutron energy.

3.1 Input Parameters

The *Transport Code* can be found in EOS:
`/eos/experiment/ntof/simul/transport`
The most updated version, to be synchronized with the evolution of the development, of the code is in a GIT repository:
`https://gitlab.cern.ch/ntof/transport`

This is the list and the short description of the input parameter to the code that

have to be provided when launching the program:

- **-?**, **--help** Help page.
- **-a**, **--angle** Angular cut [degrees].
- **-b**, **--bmin** Minimum 2D histogram y-value [eV,s,cm].
- **-B**, **--bmax** Maximum 2D histogram y-value [eV,s,cm].
- **-c**, **--tmin** Minimum time cut at measuring station to score [s].
- **-C**, **--tmax** Maximum time cut at measuring station to score [s].
- **-d**, **--data** Data file with particle distributions.
- **-D**, **--dir** Direction to propagate [XYZ].
- **-e**, **--emin** Minimum energy cutoff [eV].
- **-E**, **--emax** Maximum energy cutoff [eV].
- **-h**, **--hmin** Minimum histogram x-value [eV,s,cm].
- **-H**, **--hmax** Maximum histogram x-value [eV,s,cm].
- **-i**, **--input** Input file with collimation information.
- **-L**, **--length** Scoring distance [m].
- **-m**, **--mbins** Histogram number of bins for 2D histogram.
- **-n**, **--nbins** Histogram number of bins for 2D histogram.
- **-p**, **--particle** Particle type (def=8=neutron).
- **-P**, **--primaries** Number of primaries (def=1).
- **-r**, **--rmin** Minimum radius [cm].
- **-R**, **--rmax** Maximum radius [cm].
- **-w**, **--xSCenter** x coordinate of the scoring center (circular scoring) [cm].

- **-W**, **--ySCenter** y coordinate (z in EAR2 case) of the scoring center (for circular scoring) [cm].
- **-s**, **--rstep** Scanning step size[cm].
- **-S**, **--sigma** Sigma of Gaussian smoothing on time [s].
- **-t**, **--target** Spallation target radius [cm].
- **-T**, **--type** Histogram type ([e]nergy, [t]ime, profile[xyr2], [l]ambda).
- **-x**, **--x0** X-offset to subtract from data [cm].
- **-y**, **--y0** Y-offset to subtract from data [cm].
- **-z**, **--z0** Z-offset to subtract from data [cm].
- **-0**, **--t0** t0-offset to subtract from time [ns].
- **-u**, **--xmin** Minimum x for rectangular scoring [cm].
- **-U**, **--xmax** Maximum x for rectangular scoring [cm].
- **-v**, **--ymin** Minimum y for rectangular scoring [cm].
- **-V**, **--ymax** Maximum y for rectangular scoring [cm].
- **--rectangular** Select a rectangular as scoring region (**-u -U -v -V** needed).
- **--gravity** Applies the gravitational correction for neutrons below 10 eV.
- **--xs** <file >Sample cross section file with the energy[eV] and the cross section[barn] of the reaction.
- **--xstotal** <file >Total cross section file: energy[eV], cross section[barn].
- **--atob** Sample atomic density [atoms/barn].
- **--Sxs** <file >Support material cross section file.
- **--Satob** Support material atomic density [atoms/barn].
- **--eff** <file >Two column file with efficiency as a function of energy (eV).

Notes and clarifications on previous parameters:

- Keep the following values untouched since they are related with simulation conditions. A variation of them can lead to a systematic error in the results:
  - EAR1: **-D Z -t 40 -x 0.0 -y0.0 -z41.06**
  - EAR2: **-D Y -t 16 -x -10.8 -y37.2 -z 9.86**
- Notice that the axis for EAR1 is OZ while for EAR2 is OY with a displacement in the other two coordinates coming from the misalignment of the first pipe in the beam line with respect to the geometrical center of the target: "**-D Z**" for EAR1 and "**-D Y**" for EAR2.
- **-L** is the flight path, i.e., the distance from the center of the target to the re-sampling surface, for instance, the detector location in the experimental area. The position of the simulation scoring plane is removed internally by the routine, reason why the above parameters must be kept untouched.
- Path of FLUKA simulations in EOS (**-d**), the correct file it should be the file *EAR1.bin* or *EAR2.bin*:
  /eos/experiment/ntof/simul/phase3/data_mcnp
  In this directory the runs are divided into groups of thousands:
  00___ for runs from 1 to 999.
  01___ for runs from 1000 to 1999.
  ...
  and there is a sub-directory for each run like *0001*, *0999*, etc... Every thousand runs are combined in a global *EAR1.bin* and *EAR2.bin* file of about 250 Mb. However due to server problems there are not always 1k runs per folder and not all have the same starting primaries. The total amount of primaries **-P** that was simulated per *XX___* folder can be found inside the "info" file.
- **-o** is the output histogram for the data file. 1D histograms of counts (or reaction rates) as a function of the energy, time, spatial distribution or λ as well as the 2D version of any of them. One output file is produced for each cycle/run.
- Particle ID as in FLUKA, i.e., **-p 8** for neutrons and **-p 7** for photons.

- The *angle cut* (**-a**) is the aperture of the cone at the scoring plane defined for the optical transport. As bigger the angle, smaller the statistical fluctuations, but sampling of also unwanted particles. It can be set as 10 degrees to get the flux and the beam profile. Nevertheless, the accuracy of the RF decreases with the angle.

- Spallation target radius: **-t 40** for EAR1 and **-t 16** for EAR2.

- Beam RMS: **-S 7.e-9** for nominal proton pulses.

- The t_0 offset (**-0**) is a constant to be deduced from the TOF. In case of EAR1, t_0 is usually the equivalent in time of λ-distribution in time.

- By default, the shape of the sample is considered as circular and centered with respect to the beam axis. Rectangular samples are also accepted when **-u, -U, -v, -V** are used. The center position offset is included via **-x, -y, -z** parameters.

- Additionally, for misalignment samples **-w** and **-W** should be defined to center in a proper way the scoring center location.

- **-R** Sample radius. At 1.5 m from EAR2 floor, the maximum beam size is 2.5 cm. **-s** is the integration step in cm to scan the defined sample.

- Histogram type (**-T, --type**) refers to the magnitude to be generated with the routine [e]nergy, [t]ime, profile[xyr2], [l]ambda. On top of that, the histogram can be 1D or 2D according to the input specifications:

  -Tt Spectra in TOF. 1D-distribution.

  -Te Spectra in true-energy. 1D-distribution.

  -Ttl Spectra for lambda as a function of the TOF. It is a 2D-distribution.

  -Tl Spectra for lambda as a function of the true-energy (2D-distribution).

  -T2 Spectra in 2D, for instance, "xyr2" for the profile.

- The *input file with collimator information* (**-i**) contains the optical parameters of the vacuum chamber, i.e., includes the position and dimensions of any obstacle in the beam such as collimators or beam pipe reductions. Obtain this information from the experts or from the technical drawings. In

EOS: /eos/experiment/ntof/simul/transport/input/
based on the different possible configurations of the beam line for each experimental area such as the collimator size (small/big).

  - EAR1: *ear1misalign.inp*, *ear1fission_misalign.inp*, *ear1_5cm.inp*, *ear1_capture_2011.inp*, *ear1fission.inp*
  - EAR2: *ear2_misalign_2015.inp*, *ear2_misalign_fission_2015.inp*

- The *Transport Code* also provides the count rate estimation of a given neutron-induced reaction. In fact, the output of the code is the expected $Yield \cdot flux$. Therefore, in order to get the yield, the user should also run the program to get the flux (see Eq. 4.29) and divide both quantities. Contrary to other magnitudes, a series of additional parameters are needed: the particular cross section of the reaction (**--xs**) under study, the total cross section (n,tot) (**--xstotal**), the sample mass (**--atob**) of the isotope of interest, the total efficiency (**--eff**) of the experiment, i.e., including all energy-depending factors such as the geometrical detector efficiency or the effect of the angular distribution of the reaction with neutron energy, and the transmission factor which is calculated internally by the code using the provided (n,tot) cross sections (**--Sxs**) of each of the isotopes present in the material intercepting the beam as well as their atomic densities (**--Satob**). All the files should be in text-format with two columns: the first one with the neutron energy and the second one with the value of the magnitude at the specific energy in ideal conditions since the code will do the convolution with the RF in order to reproduce the experimental conditions.

The code is run for a single FLUKA simulation output or for several of them. There are available a set of routines, written in python, to merge the individual outputs to a single one, properly treating the statistical uncertainties. The final output is a text file that can be converted to a ROOT file to process in a more easy way the generated histograms. Below, several example are shown as if the program were running directly by the user on LXPLUS in the directory where all the required files as input are located, except for the simulation outputs, including the *Transport Code* executable. Nevertheless, the use of the GUI is highly recommended (see Section 3.2) since the user can launch the *Transport Code* and

post-process the output files getting directly the final root file.

Important note: the term *neutron energy* always apply to the "true-energy" of neutrons, i.e, the energy that neutrons would have at the production point NOT the one from the TOF to energy conversion. The second one is affected by the RF while the first one do not. For the calculation of the expected count rate, the text files should contain the true-energy which is folded with the RF to get TOF comparable with the measured TOF.

3.1.1 Examples

- EAR2 neutron flux in TOF for big collimator:
  ./transport -d /eos/experiment/ntof/simul/phase3/data_mcnp/00___/EAR2.bin -P9510000 -o out/res_0.hist -i ear2_misalign_fission_2015.inp -DY -t16 -x -10.8 -y37.2 -z9.86 -p8 -a10 -S7e-09 --t0 0.0 -r0.0 -R10.0 -s0.05 -L19.5 -Tt -h1e-12 -H1e0 -n6000

- EAR1 beam profile for neutron energies from thermal to 0.1 eV:
  ./transport -d /eos/experiment/ntof/simul/phase3/data_mcnp/00___/EAR1.bin -P9510000 -o ThXY.out -i ear1_5cm.inp -DZ -t40 -x0.0 -y0.0 -z41.06 -S7.e-9 -p8 -a5 -L185.0 -R2.1 -s0.01 -T2 -e25.e-3 -E1.e-1 -n250 -m250

- EAR2 lambda as a function of the TOF:
  ./transport -d /eos/experiment/ntof/simul/phase3/data_mcnp/00___/EAR2.bin -P951000000 -o data_L/TL_ear2.out -DY -t16 -x-10.8 -y37.2 -z9.86 -S7.e-9 -p8 -Ttl -h1e-7 -H1.e-2 -n100 -b0 -B100 -m100 -L19.085 -R2.5 -s0.1 -a2.5

- EAR2 lambda as a function of the true-neutron energy:
  ./transport -d /eos/experiment/ntof/simul/phase3/data_mcnp/00___/EAR2.bin -P951000000 -o data_L/TE_ear2.out -DY -t16 -x-10.8 -y37.2 -z9.86 -S7.e-9 -p8 -TL -h1e-3 -H1.e9 -n300 -b0 -B100 -m100 -L19.085 -R2.5 -s0.1 -a2.5

- $^{197}Au(n,\gamma)$ expected count rate at EAR2 with small collimator:
  ./transport -d /eos/experiment/ntof/simul/phase3/data_mcnp/00___/EAR2.bin -P951000000 -o out/res_0.hist -i ear2_misalign_revised2018.inp -DY -t16 -x -10.8 -y37.2 -z9.86 -p8 -a2.5 -S 7e- 9 --t0 0.0 -r0.0 -R2.0 -s0.05 -L19.5

-Te -n1200 -h1.00E-03 -H1.00E+09 --xs 197Au_ng_ENDF-VIII-0.txt --atob 0.000147497 --xstotal 79-Au-197_tot.xs --eff eff.dat

3.2 Launch the *Transport Code* through the GUI

A GUI was developed with the aim of making more user-friendly the use of the *Transport Code*. The idea behind is to provide a powerful tool that guides the user through all the possible options of the code without the need of having a deep knowledge about the code itself and simulation details. The GUI is also capable of post-processing the output files, in text format, and gives the desirable ROOT files. The User's Guide can be found in the n_TOF TWiki web page:
https://twiki.cern.ch/twiki/bin/view/NTOF/TransportCode

The GUI has three functionalities: *Launch simulations*, though this option the user can define the parameters of a new simulation and can submit them; *Check the status* of the already launched simulations; and *Create plots*, i.e., convert the data output files into ROOT files. Please, check the User's Guide for a detailed explanation.

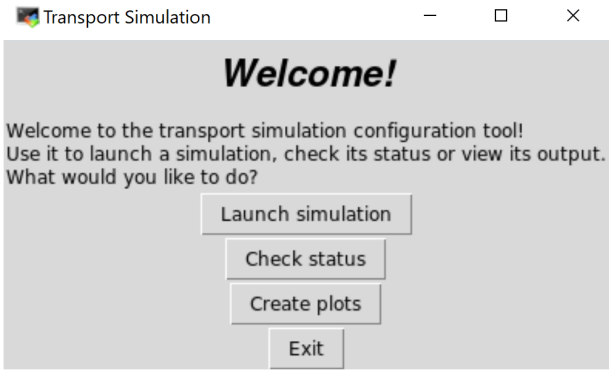

Figure 3.3: GUI Welcome Screen

The location in AFS (on LXPLUS) of the source code and the executable is:
/afs/cern.ch/user/n/ntofsimu/public/transport/GUI/transport_gui/
Launching the GUI is very simple, just go to your working directory, type the following command and enjoy the experience:
python /afs/cern.ch/user/n/ntofsimu/public/transport/GUI/transport_gui/App.py

3.3 How to obtain the numerical RF (UDR) as input for SAMMY/REFIT

The code *RF2sammy.C* transforms a two-dimensional resolution function into a form that can be used by the resonance shape analysis codes SAMMY and REFIT. It requires a ROOT file containing a TH2 histogram as is typically given as output by the *Transport Code*. A valid installation of ROOT is also needed. The TH2 histogram needed by *RF2sammy* is expected to have axes in energy (units: eV), and in equivalent distance (units: cm). Conversion options can be invoked when the units in the input file are different.

The source code *RF2sammy.C* is available at:
/eos/experiment/ntof/src/RF2sammy/
that contains compilation and operation instructions in the preamble.
A compiled executable is on lxplus at:
/eos/experiment/ntof/bin/RF2sammy

A number of arguments has to be given to *RF2sammy*, of which two are mandatory: the filename and the name of the TH2 histogram it contains, the others are optional. The most straightforward way to run on lxplus, assuming that /eos/experiment/ntof/src/bin/ is in your search path, is the following:

RF2sammy -i <rootfile_name> -t <histogram_name>

This will result in a single text output file suited for inclusion with SAMMY (default) or REFIT (use flag '-R'). The name of the output file is just that of the input file with "_SAMMY_UDR.txt" or "_REFIT_UDR.txt" appended to it. The optional arguments allow for the scaling of the TH2 input energy and distance units, for the possible grouping of bins, or for the production of plots (option '-p 1'). The full list of options is shown when *RF2sammy* is called without options. At present this lists:

Mandatory arguments:

- **-i** input filename.
- **-t** histogram name.

Optional arguments:

- **-o** output filename, default: *input filename + '_SAMMY_UDR.txt'*.
- **-w** enlarge (number of bins around energy slice), default: 1.
- **-m** group energy bins in TH2, default: 1 bins.
- **-n** group distance bins in TH2, default: 1 bins.
- **-s** smooth parameter, default: 0.
- **-p** 1: produce plots.
- **-f** scaling factor to convert TH2 energy to eV, default: 1.0.
- **-d** scaling factor to convert TH2 distance to cm, default: 1.0.

Optional flags:

- **-z** test.
- **-c** use classical energy-time relation. Default is relativistic.
- **-R** use REFIT output. Default: SAMMY output.

Chapter 4

Appendix: Yield calculation using the re-sampling method

4.1 Time-of-flight technique

The time-of-flight or TOF is a technique to determine the energy of neutrons from the time they spend traveling a given flight path, i.e., the distance between the spallation target and the front face of the detector system located in the experimental hall. In a pulsed neutron beam, a collection of neutrons with different kinetic energies is produced and slowed down by passing through a moderator. The arrival time of each neutron is connected to their velocity by means of the geometrical distance, L_0: $v = L_0/TOF$, and the kinetic energy of a single neutron, E_n, is given by:

$$E_n = E - m_n c^2 = \sqrt{c^2 p^2 + m_n^2 c^4} - m_n c^2 \tag{4.1}$$

being c the speed of light, m_n the rest mass of the neutron and $p = m_n \cdot v \cdot \gamma$ the momentum of the neutron, where $\gamma = \frac{1}{\sqrt{1-v^2/c^2}}$ is the Lorentz factor. Thereby:

$$E_n = m_n c^2(\gamma - 1) = m_n c^2 \left(\frac{1}{\sqrt{1 - (L_0/(TOF \cdot c))^2}} - 1 \right) \tag{4.2}$$

Eq. 4.2 is the relativistic relationship between the kinetic energy and the time-of-flight. Below few tens of MeV, the relativistic effects can be neglected and the first term of the Taylor series expansion can be kept in order to obtain the classical formula. Taking c=*299.8 m/μs* and the neutron mass as m_n=*939.6 MeV/c^2*:

$$E_n = \frac{1}{2} m_n v^2 = \left(\frac{72.29 \cdot L_0}{TOF} \right)^2 \tag{4.3}$$

where TOF is the true time-of-flight of a neutron traveling from the outer surface of the spallation target to the experimental area defined as the difference between the measured time-of-flight, t_m, and the moderation time, t_{mod}. The first one is in turn the acquired time for an event minus a reference time known as t_0:

$$TOF = t_m - t_{mod} = (t - t_0) - t_{mod} \tag{4.4}$$

The γ-flash is the first signal observed in the majority of measuring stations at a time t_γ. On top of that, the time that photons are traveling is L_0/c. Therefore, the time stamp for the spilling of the protons in the spallation target becomes: $t_0 = t_\gamma - L_0/c$, and then:

$$TOF = t_m - t_{mod} = (t - t_\gamma) + \frac{L_0}{c} - t_{mod} \tag{4.5}$$

In Figure 4.1 a scheme of the TOF determination method at n_TOF is shown.

On the other hand, the moderation time can be treated as a virtual length, λ, which is the effective distance at the time of the evaluation mostly determined by the last collisions during the moderation process:

$$v = \frac{L_0}{TOF} = \frac{L_0}{t_m} \cdot \frac{t_m}{TOF} = \frac{L_0}{t_m} \cdot \left(1 + \frac{t_{mod}}{TOF} \right) = \frac{L_0 + \lambda}{t_m} \tag{4.6}$$

hence:

$$\lambda = L_0 \cdot \frac{t_{mod}}{TOF} = v \cdot t_{mod} \tag{4.7}$$

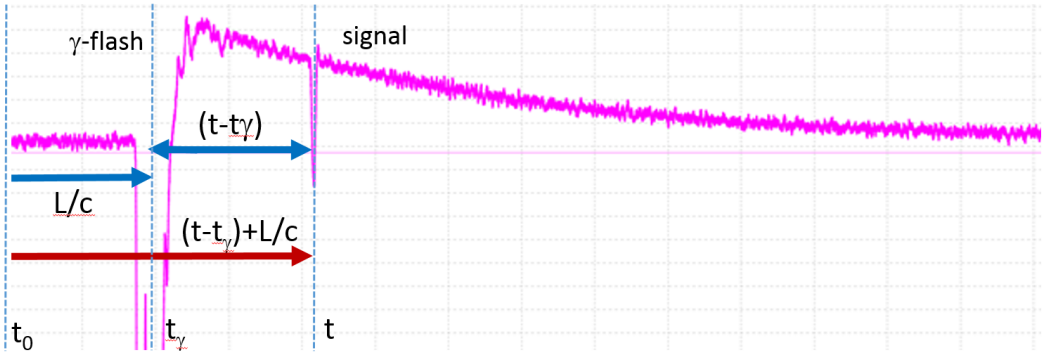

Figure 4.1: Scheme of the technique to define the value of t_m. The recorded time of a signal with the DAQ, t, is not the time-of-flight of the neutron that induced the reaction. In order to get a proper t_m, a reference time is defined as the arrival time of the γ-flash, t_γ, corrected by the time spends by photons in the beam line, L_0/c.

Accordingly, Eq. 4.2 can be rewritten as:

$$E_n = m_n c^2 \left(\frac{1}{\sqrt{1 - \left(\frac{L_0+\lambda}{c \cdot t_m}\right)^2}} - 1 \right) \tag{4.8}$$

λ is a stochastic quantity described by means of a probability density on the neutron energy known as response function which is related with the energy resolution of the facility. Monte Carlo simulation is the most suitable way for estimating this distribution which only depends on the neutron production mechanism, the size of the target and the cooling/moderation system [15]. The elastic scattering is the essential process in neutron moderation while inelastic scattering can be safely neglected in the calculation (see Section 4.2).

Besides, the energy resolution of incoming neutrons, ΔE, is the capability of resolving resonance structures in the cross section which is related to the velocity resolution, Δv, in a time-of-flight spectrometer [2, 16]:

$$\frac{\Delta E}{E} = (\gamma + 1) \cdot \gamma \cdot \frac{\Delta v}{v} = (\gamma + 1) \cdot \gamma \cdot \sqrt{\left(\frac{\Delta T}{T_{rms}}\right)^2 + \left(\frac{\Delta L}{L}\right)^2} \tag{4.9}$$

wherein Δ refers to the standard-deviation and T_{rms} is the r.m.s. of the beam. At low velocities when the relativistic expression for kinetic energy of neutrons can be approximated by the classical one (Eq. 4.3), $\gamma \approx 1$ and:

$$\frac{\Delta E}{E} = 2 \cdot \sqrt{\left(\frac{\Delta T}{T}\right)^2 + \left(\frac{\Delta L}{L}\right)^2} \tag{4.10}$$

Fluctuations in the flight path are mainly due to variations in λ, $\Delta L \approx \Delta\lambda$, while fluctuations in time is related to the proton bunch width, $\Delta T = 7 - 20$ ns depending on the type of proton pulse sent by the PS. Obviously, the use of longer flight path and the production of neutrons in short bunches, small ΔT and ΔL, benefit the energy resolution of the facility.

4.2 Moderation and Response Function

n_TOF is a spallation neutron source based on a proton beam of 20 GeV/c momentum generated at the CERN-PS, impinging onto a 1.3 tonne cylindrical lead block of 40 cm in length and 60 cm in diameter. Protons of the incoming beam deposit a fraction of their energy in the target via incoherent nucleon-nucleon collisions, starting the intra-nuclear cascade that decays by successive emission of nucleons and pions. The probability to undergo this process is given by the relative geometrical cross section of the particles involved, i.e., the relativistic proton and lead nuclei. After a pre-compound stage, in which nucleons and light clusters are emitted, the de-excitation of the residual nucleus goes forward via multi-fragmentation, Fermi breakup, fission and evaporation of nucleus and light clusters followed finally by photon evaporation and radioactive decay. Under n_TOF operation conditions, about 300 neutrons per incident proton of 20 GeV/c momentum are yielded via spallation process. Most of them have high energy. Therefore, in order to enlarge the neutron energy range of the spallation neutron source, the use of a moderator becomes very important to slow down fast neutrons and populate the neutron energy spectrum down to thermal.

Energy - Time relationship [17]

The quantity $ln(E_1/E_2)$ is called *lethargy* that represents the *average logarithmic energy* loss per collision:

$$\xi = \overline{ln\frac{E_1}{E_2}} = 1 + \frac{a}{1+a} \cdot lna \tag{4.11}$$

Taylor approximation gives for $A > 1$:

$$\xi \approx \frac{2}{A + \frac{2}{3}} \tag{4.12}$$

This is a good approximation for $A \geq 10$ while for $A = 2$ there is an error of 3%. For mixtures:

$$\overline{\xi} = \frac{\Sigma_i N_i \cdot \sigma_s^i \cdot \xi_i}{\Sigma_i N_i \cdot \sigma_s^i} \quad where \quad \sigma_s \quad is \quad the \quad scattering \quad cross-section. \tag{4.13}$$

The lethargy can be used to estimate the number of collisions to moderate from the initial energy E_i to E_f:

$$n \cdot \xi = ln\frac{E_i}{E_f} \tag{4.14}$$

Then, the neutron fluence depends on the slowing down power, $\overline{\xi} \cdot \Sigma_s$, and the moderation ratio, $\xi \cdot \Sigma_s / \Sigma_a$ where Σ_a is the macroscopic absorption cross section:

$$\Phi(E) = \frac{C}{\overline{\xi} \cdot \Sigma_s \cdot E} \tag{4.15}$$

For larger ξ, faster the slow down. And for larger Σ_s, the macroscopic scattering cross section, more often the collisions will be.

During moderation, the average increase in lethargy, i.e., $u = n \cdot \xi$ is:

$$\frac{du}{dt} = \xi \cdot \Sigma_s \cdot \frac{dx}{dt} = \xi \cdot \Sigma_s \cdot v \tag{4.16}$$

Considering Eq. 4.14: $v_f = v_i \cdot e^{-\frac{u}{2}}$. Therefore:

$$\frac{dv}{dt} = -\frac{\xi \cdot \Sigma_s}{2} v^2 \tag{4.17}$$

Integrating:

$$t = \frac{2}{\xi \cdot \Sigma_s} \int_v^{v_0} \frac{dv}{v} = \frac{2}{\xi \cdot \Sigma_s} \left(\frac{1}{v_f} - \frac{1}{v_i} \right) \tag{4.18}$$

Then, converting to energy:

$$E = \frac{2 \cdot m_n}{(\xi \cdot \Sigma_s \cdot t)^2} v(t) \tag{4.19}$$

For $A = 1$:

$$\overline{E(t)} = \frac{3 \cdot m_n}{(\Sigma_s \cdot t)^2} = \frac{1.8 eV \mu s^2}{t^2} \tag{4.20}$$

For $A >> 1$:

$$\overline{E(t)} = \frac{m_n}{2} \cdot \frac{A \cdot (A+2)}{(\Sigma_s \cdot t)^2} \approx \frac{A^2}{(\Sigma_s \cdot t)^2} \cdot 0.522 eV \mu s^2 cm^{-2} \tag{4.21}$$

More accurately [18]:

$$\overline{E(t)} = \frac{K}{(t + t_0)^2} \tag{4.22}$$

where $K = m_n \cdot \lambda_s^2 \cdot (1-a)^2/(2a^2)$ and $t_0 = (1-a)(\lambda_s/a)\sqrt{m_n/(2 \cdot E_0)}$. Eq. 4.22 is the neutron energy at time t from the moderation process. While the energy at after flying a length equal to L_0 is:

$$E = \frac{m_n \cdot L_0^2}{2 \cdot t^2} \tag{4.23}$$

Relativistically:

$$\gamma = \frac{1}{\sqrt{1 - (L_0/(t \cdot c))^2}} \quad then \quad E_{kin} = (\gamma - 1) \cdot m_n \tag{4.24}$$

Differentiating we can get the uncertainty:

$$\frac{\Delta E}{E} = -2\frac{\Delta t}{t} = 2\frac{\Delta \lambda}{L_0 + \lambda} \tag{4.25}$$

where λ is a virtual quantity called *effective neutron path*. The neutron velocity, v, is derived from the *effective neutron path*: $v = (L_0 + \lambda)/t$ with an uncertainty $\Delta v = \Delta\lambda/t$ (see Figure 4.2). It is extremely important to not confuse this *effective neutron path* with the *moderation path*.

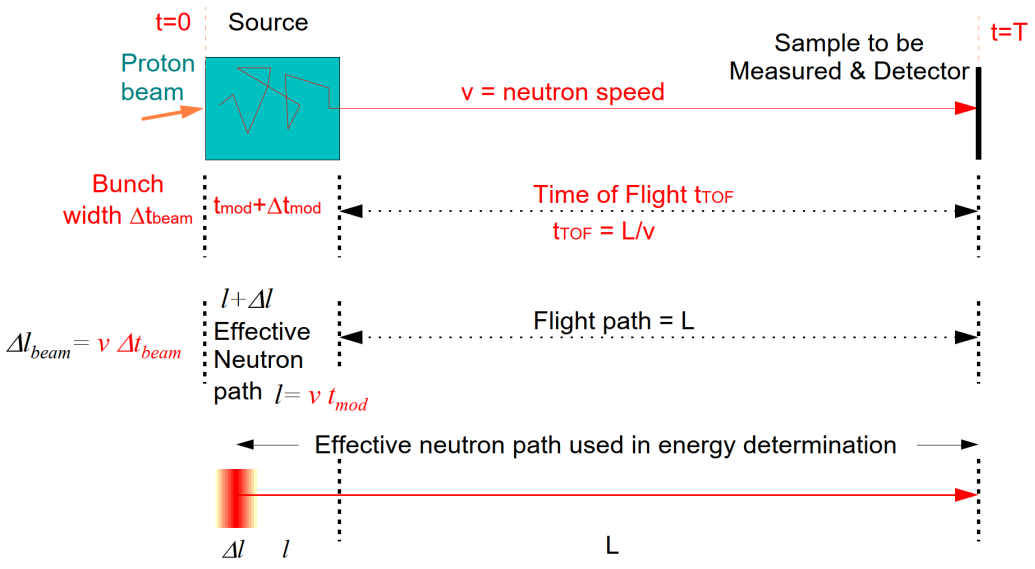

Figure 4.2: Scheme of neutron velocity and effective neutron path calculation. In this representation: $l = \lambda$.

Neutron moderation [17]

The mean free path of a neutron inside an extensive target is given by:

$$\lambda_s = \frac{1}{\Sigma_s} = \frac{1}{\sigma_s \cdot \rho \cdot (N_A/A)} \approx const. \tag{4.26}$$

The velocity and time after n-collisions are given by:

$$v_n = v_1 \cdot exp\left(-\xi \cdot \frac{n-1}{2}\right) \quad , \quad t_n = \frac{\lambda_s}{v_1} \cdot \sum_{i=1}^{n} exp\left(\xi \cdot \frac{i-1}{2}\right) \tag{4.27}$$

Taking into account that the average energy loss in collisions is given by Eq. 4.12, the effective length (λ_n) after n-collisions is:

$$\lambda_n = v_n \cdot t_n = v_1 \cdot exp\left(-\xi \cdot \frac{n-1}{2}\right) \cdot \frac{\lambda_s}{v_1} \cdot \sum_{i=1}^{n} exp\left(\xi \cdot \frac{i-1}{2}\right) \approx 2 \cdot \frac{\lambda_s}{\xi} \tag{4.28}$$

Figure 4.3 shows a scheme of the process by which neutrons lose their energy; in addition, the neutron energy versus time at the target window and at the detector location is also shown. Table 4.1 presents the *effective neutron path* for different material of interest in the case of n_TOF: *lead* which is the target material, *aluminium* for the target windows and *water* for the moderator and cooling system. The last two columns of the table are related to the spread of the *effective neutron path* that it is determined by the energy loss after the collision (Figure 4.4).

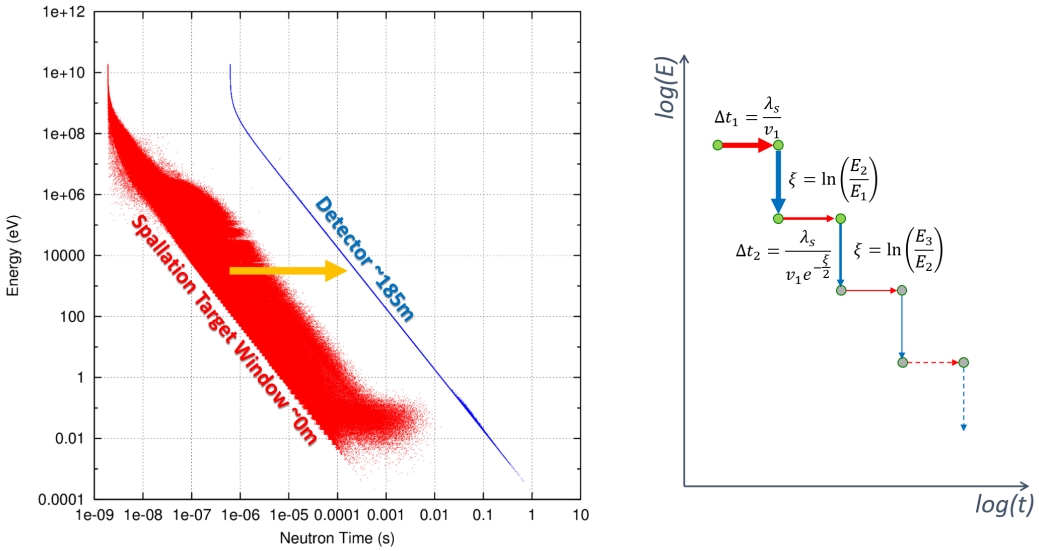

Figure 4.3: Left: Neutron energy versus time at the target window (red) and at the detector location (blue). Right: Scheme of the process by which neutrons are losing their energy (ξ) after each collision in the media, the velocity of neutrons decreases as shown in Eq. 4.27.

Material	σ_s **(1KeV) [b]**	λ_s **[cm]**	ξ	λ **[cm]**	$\sqrt{(\Delta E/E)^2}$	$\Delta\lambda$ [cm]
Lead	11.35	2.7	$9.6 \cdot 10^{-3}$	560	11.4%	32
Aluminium	1.42	11.7	$7.2 \cdot 10^{-2}$	320	31.4%	53
Water		0.67		1.5	150%	2.25
H	$\sigma_s(H)$=20.3		$\xi(H)$=1			
O	$\sigma_s()$=3.85		$\xi(O)$=0.12			

Table 4.1: Information needed to calculate the effective neutron path for different materials. The λ-values correspond to the maximum of the λ distribution and $\Delta\lambda$ to the spread of the peak (See Figure 4.4).

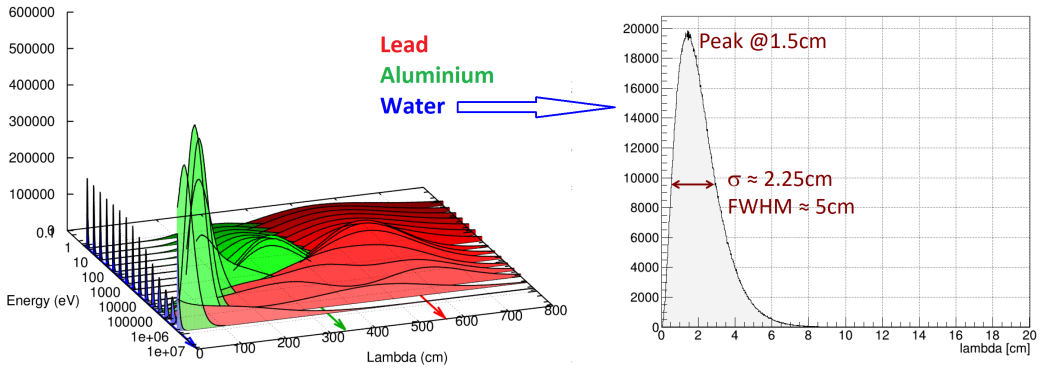

Figure 4.4: Left: Effective neutron path or λ distribution as a function of the neutron energy for different materials. On the right it is shown the projection of the distribution for the case of water: the parameters in Table 4.1 are presented here as the peak and sigma of the distribution at a given energy.

4.3 TOF to Energy calibration

In view of what has been exposed before, the TOF to energy conversion is based on two assumptions: the knowledge of the L_0 and the λ distribution. The most widely used method to calculate the L_0 is by means of fitting the lowest energy resonances of the ^{235}U(n,f) cross section, i.e., matching the position in time-of-flight of the measured cross section with the position in energy included in the evaluation for the same reaction. Other reactions can be used as well, this will depend on the reference sample chosen for the measurement. In case of EAR2 the effect of the moderation length cannot be neglected as illustrated in Figure 4.5, where the black line represents the ^{235}U(n,f) yield considering the ENDF/B-VII.1 evaluation and the red line is the same yield folded with the n_TOF-EAR2 resolution function. The shift in energy between the two curves for the first resonance is quite small but for the rest it becomes gradually worse with the neuron energy.

A more accurate procedure has been recently developed at CERN which takes into account the whole λ-distribution to make the convolution instead of an approximation of it, such as the maximum or the mean value of the distribution. As mentioned before, spallation processes are replicated via Monte Carlo simula-

tions. Neutrons produced are scored to a plane located at certain distance from the center of the spallation target, 37.2 cm in case of FLUKA and 150 cm in case of GEANT4 [19]. Those neutrons are tagged with the energy at the production point, or equivalently true-energy, and its time-of-flight from the moment they are generated to the time they reach the scoring position. By means of performing an optical transport, i.e., a re-sampling of neutrons from the original scoring position given by simulations to the desirable location, for instance the experimental hall, the time-of-flight changes accordingly to the path that neutrons fly, while the true-energy remains unchanged.

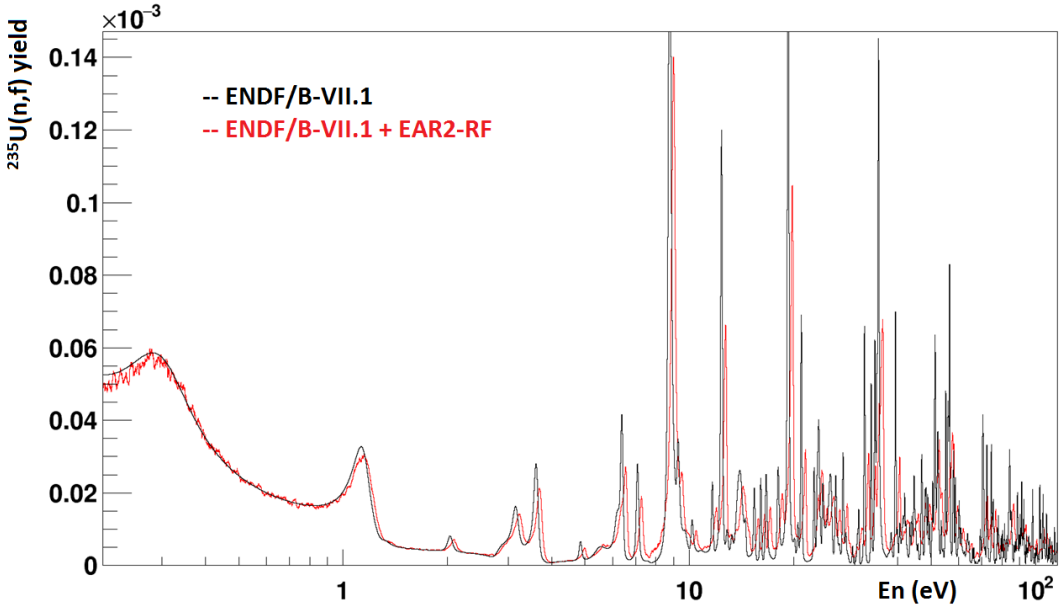

Figure 4.5: Comparison of the yield for $^{235}U(n,f)$ considering ENDF/B-VII.1 evaluation (black) and the same yield convoluted with the resolution function of EAR2 (red). There is a visible shift between the two that becomes gradually bigger with the increasing neutron energy [8].

In order to get the yield, the total and partial cross section of the reaction under study as well as the areal density of the sample, the efficiency of the detection system, the cross section and areal density of any material in-beam as function of the energy should be given as input parameters to the *Transport Code*. The routine will then provide the count rate ($Yield \cdot \Phi$) corrected by all

the factors mentioned before and the simulated flux (Φ) re-sampled to the final scoring surface:

$$Yield_{ENDF+RF}(TOF) = \frac{\int Yield_{ENDF+RF}(TOF, E) \cdot \Phi_{sim}(TOF, E) \cdot dE}{\int \Phi_{sim}(TOF, E) \cdot dE} \tag{4.29}$$

where $Yield_{ENDF+RF}(TOF)$ is the expected yield based on the evaluation used as input. In this case, the integral is made throughout the entire energy spectrum but it can be made in the same way in TOF to get $Yield_{ENDF+RF}(E)$, where E is the true-energy of neutrons. On top of that, the lack of statistics also leads to a deformation on the shape of the convoluted function when folding directly the cross section with the λ-distribution as it is shown in Figure 4.6 left, while using re-sampling and the transport routine those fluctuations can be avoided (check Figure 4.6 right), revealing the potential of the procedure.

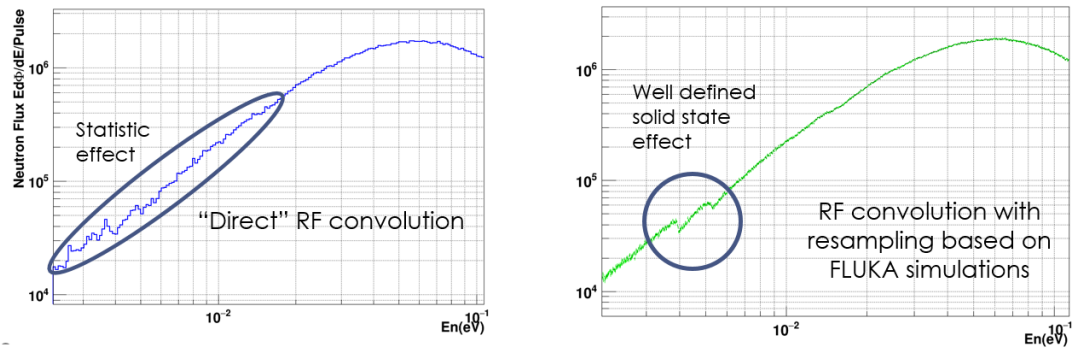

Figure 4.6: Comparison of two convolution methods. On the left, a explicit λ-distribution is included hence the lack of statistic in the distribution is propagated to the resulted function. While on the right, the same convolution is shown this time using the Transport Code. The fluctuations are not visible anymore and the structure that was hidden within them becomes visible [8].

A direct comparison of the resonance position in TOF is now possible avoiding any kind of fit. Of course, the parameter to be found is the position of the re-sampling plane with respect to the spallation target being the first guess the value obtained via the procedure explained at the beginning of this section, what leads to an iterative process. λ depends on the scorer selected during the simula-

tion thus it is more appropriate to describe the flight path length as $L_0+\lambda(TOF)$ instead of $L_0 + \lambda$ in Eq. 4.8, being L_0 the geometrical distance between the two scoring surfaces. In those cases in which the statistical fluctuations of the simulations are too big for extracting the projection of the λ-distribution, an effective flight path can be used instead in the TOF to energy conversion, L, which includes an average impact of the resolution function. For instance, the expected count rate at the measurement position of ^{235}U(n,f) based on the ENDF data library is obtained in time-of-flight as shown in Figure 4.7 together with the experimental count rate. The agreement between the two is rather good for most of the resolved resonances.

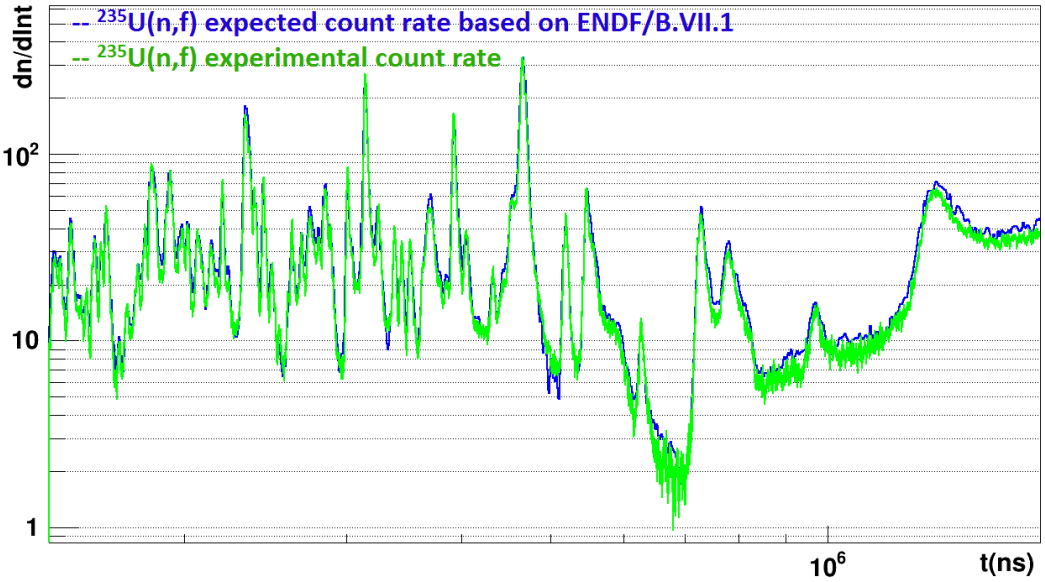

Figure 4.7: Expected count rate based on ENDF/B-VII.1 nuclear data library for the ^{235}U(n,f) reaction convoluted with the n_TOF-EAR2 resolution function by means of the transport routine (blue) in comparison with the experimental count rate for the same reaction (green) as a function of the time-of-flight. The agreement in the resonance position is very satisfactory [8].

For those reactions without resonances, the geometrical distance between the ^{235}U sample position and the converter of interest is added. The time-of-flight to energy conversion relies on Monte Carlo simulations what introduces a 2 - 5 % systematic uncertainty all over the energy range.

Bibliography

[1] www.cern.ch/ntof (2)

[2] C.Guerrero *et al.*, *Performance of the neutron time-of-flight facility n_TOF at CERN*, Eur. Phys. J. A **49** (2013) 27. (2, 36)

[3] N. Colonna, F. Gunsing, E. Chiaveri, *The Second Beam-Line and Experimental Area at n_TOF: A New Opportunity for Challenging Neutron Measurements at CERN*, Nuc. Phys. News, **25**:4, 19-23 (2015). (2)

[4] N.M. Larson, *Updated users guide for SAMMY: Multilevel R-matrix fits to neutron data using Bayes' equations*. Report ORNL/TM-9179/R8 and ENDF-364/R2, Oak Ridge National Laboratory, USA, (2008). (2)

[5] M.C. Moxon and J.B. Brisland, *GEEL REFIT, A least squares fitting program for resonance analysis of neutron transmission and capture data computer code*. AEAInTec-0630, AEA Technology, October (1991). (2)

[6] https://fluka.cern/ (3, 6)

[7] C. Weiss *et al.*, *The new vertical neutron beam line at the CERN n_TOF facility design and outlook on the performance*. NIM A **799** 90 (2015). (4)

[8] M. Sabaté-Gilarte, *PhD Thesis: The n TOF-EAR2 facility at CERN: neutron flux determination and $^{33}S(n,\alpha)^{30}Si$ cross section measurement; implications in BNCT*. https://cds.cern.ch/record/2711650/files/CERN-THESIS-2017-481.pdf. (4, 5, 23, 44, 45, 46)

[9] *MCNPX Users Manual, Version 26d. LA-UR-07-4137 (2007).* (6)

[10] V. Vlachoudis *et al.*, *EAR2 Resolution Function. Update on FLUKA+MCNPx simulations.* https://indico.cern.ch/event/844622/contributions/3546550/attachments/1918258/3172487/Resolution_Function_2019-10.pdf (6, 11)

[11] F. Ogallar Ruiz *et al.*, *EAR2 Energy Resolution Function. Simulation updates.* https://indico.cern.ch/event/767271/contributions/3192641/attachments/1759579/2854343/RF_nTOF_Nov18_Granada_v2.pdf (6, 7)

[12] V. Alcayne, *PhD Thesis: Measurement of the Cm-244 and Cm-246 neutron-induced cross sections at the n_TOF CERN facility.* (13)

[13] V. Alcayne, E. Mendoza and the RF working group, *The RF for small samples in EAR2.* https://indico.cern.ch/event/920196/contributions/3891422/attachments/2054907/3446398/20_07n_RF_TOFCM_VIRTUAL_V04.pdf (13)

[14] I. Bergstrom, *Minimizing the background radiation in the new neutron time-of-fight facility at CERN. FLUKA Monte Carlo simulations for the optimization of the n_TOF second experimental line.* Master Thesis. CERN-THESIS-2013-203 (05/06/2013). (22)

[15] V. Vlachoudis *et al.*, *Resolution Function. Update on FLUKA simulations.* https://indico.cern.ch/event/458295/contributions/1129319/attachments/1196931/1745232/Resolution_Function_Dec_2015.pdf (36)

[16] P. Schillebeeckx *et al.*, *Determination of Resonance Parameters and their Covariances from Neutron Induced Reaction Cross Section Data*, Nuclear Data Sheet **113** 3054-3100 (2012). (36)

[17] V. Vlachoudis, *n_TOF facility, moderation and response function. Neutron Field Theory.* https://indico.cern.ch/event/677259/contributions/2815150/attachments/1585765/2507230/Vassilis_Zermatt2018.pdf (23, 38, 41)

[18] R.E.Slovacek *et al.* Nucl. Sci. and Eng. **62**:445-462,1977. (39)

[19] J. Allison *et al.*, *Recent developments in Geant4*. Nucl. Instr. and Meth. A **835** 186-225. FERMILAB-PUB-16-447-CD (2016). (44)